https://doi.org/10.5194/se-2021-68
Preprint. Discussion started: 19 May 2021

Solid Earth Discussions

Detrital zircon provenance record of the Zagros mountain building from the Neotethys obduction to the Arabia-Eurasia collision, NW Zagros fold-thrust belt, Kurdistan region of Iraq

Renas I. Koshnaw[1*], Fritz Schlunegger[1], Daniel F. Stockli[2]

[1]Institute of Geology, University of Bern, Baltzerstrasse 1+3, CH- 3012 Bern, Switzerland
[2]Department of Geological Sciences, Jackson School of Geosciences, University of Texas at Austin, Austin, TX 78712, USA

Correspondence to: Renas I. Koshnaw (renas.i.koshnaw@gmail.com)

*Present address: Department of Structural Geology and Geodynamics, Geoscience Center, University of Göttingen, Goldschmidtstraße 3, 37077 Göttingen, Germany

Abstract. Recognition of new angular unconformity and synthesizing of new detrital zircon U-Pb and (U-Th)/He provenance records, including zircon (U-Th)/(He-Pb) double dating, from the NW Zagros elucidate the basin dynamics of the foreland wedge-top and intermontane units, as well as the tectonic processes in the source terranes in response to different geodynamic phases. In this contribution, we present field observations and detrital zircon provenance data from hinterland basins to reconstruct the basin dynamics and the underlying tectonic controls in the NW Zagros in the Kurdistan region of Iraq. Results reveal that the deposition of the suture zone units of the Red Beds Series (RBS; Suwais Group, Govanda Formation, Merga Group) occurred in an intermontane basin on top of folded Upper Cretaceous units with an angular unconformity. The RBS provenance data point at the Paleogene Walash-Naopurdan-Kamyaran (WNK) arc-related complex as a source area and show substantial decrease of magmatism by ~36 Ma, as reflected by the youngest ages peaks. New detrital zircon provenance data from the hinterland wedge-top units of the proto-Zagros foreland basin (the Tanjero, Kolosh, and Gercus Formations) exhibit exclusive derivation from the Upper Cretaceous Neotethys ophiolitic terranes, different from the provenance of the older Lower Cretaceous and Paleozoic units that are dominated by the Paleozoic and Neoproterozoic age spectra. These shifts in provenance between different tectonostratigraphic units argue for sediment route reversal from E to W in response to ophiolite obduction, arrival of the WNK complex, and commencement of the continental collision during the late Eocene, followed by deposition of the RBS in the hinterland of the proto-Zagros fold-thrust belt, and paleodrainage connection with the post-collisional Neogene foreland basin.

https://doi.org/10.5194/se-2021-68
Preprint. Discussion started: 19 May 2021


Solid Earth Discussions

1 Introduction

In sedimentary basins adjacent to collisional mountain belts, synorogenic clastic deposits potentially provide information on the geodynamic setting prior to and during the collisional tectonic processes. Understanding the causes and consequences of mountain building processes is critical for the reconstruction of paleogeography, paleoclimate, and for the understanding of the long-term deformation and erosion history (Molnar and England, 1990; Avouac and Burov, 1996; Najman et al. 2010, Norton and Schlunegger, 2011; Avouac et al., 2015). Hinterland basins, such as wedge-top and intermontane basins are considered as valuable archives for the assessment of the exhumation and unroofing history of the adjacent uplifted terranes because of their proximity to the source areas. Previous research on the hinterland basins in the Andes and the Himalaya contributed to the shaping of our understanding about the evolution of ocean-continent subduction zones and continent-continent collisional zones (Horton et al., 2012; Liu et al., 2013; DeCelles et al., 2015). Nevertheless, well-preserved ancient stratigraphic successions are scarce due to the deformation of sedimentary strata as orogenesis proceeds (Horton et al., 2012; Orme et al., 2015). A possible approach to overcome this drawback is the utilization of the geochronologic and thermochronologic records preserved by detrital zircons to constrain and quantify the tectonic processes that are associated with the evolution of a sedimentary basin to identify the governing geodynamic mechanisms (Cawood et al., 2012; Colleps et al., 2020; Webb et al., 2013; Gehrels, 2014).

The Zagros fold-and thrust belt is a prominent collisional orogen on Earth that stretches for ~2000 km across the Middle East (Fig. 1a). This orogenic belt formed during the Late Cretaceous and Cenozoic due to the obduction of the Neotethys oceanic plate onto the Arabian continental plate. This was then superseded by the collision of the Arabian and Eurasian continental plates (Dewey et al., 1973; Hempton, 1985; Dercourt et al., 1986). This protracted convergence history resulted in an amalgamation of deferent tectonic terranes and in multiple deformation phases along the suture zone, overprinting the preceding tectonic configurations. As a result, uncertainties have been associated with paleotectonic models particularly for the NW Zagros suture zone. This partially explains why several subduction zones, a mantle plume and different loci for specific terranes (e.g., the Walash-Naopurdan-Kamyaran arc-related units) and key sedimentary successions (e.g., the Red Beds Series) have been inferred upon reconstructing the evolution of the NW Zagros suture zone (e.g. Numan et al., 1997; Karim et al., 2008; Al-Qayim et al., 2012; Azizi et al., 2013; Whitechurch et al., 2013; Ali et al., 2014, 2019; Moghadam et al., 2020). Similarly, also because of complexity of the convergence history, various timing of collision has been suggested (e.g. Zhang et al., 2016, Fig. 2) with a conceivable minimum age during the late Oligocene (Koshnaw et al., 2019).

This research aims at constraining the Arabia-Eurasia convergence history based on U-Pb ages of detrital zircons that are collected from the Red Beds Series deposits, below the Main Zagros fault. The target deposits occur in the NW Zagros hinterland basins in the Kurdistan region of Iraq and in the wedge-top deposits of the proto-Zagros Tanjero, Kolosh, and Gercus Formations (Fig. 1b). We will combine the new provenance information with published data from the wedge-top deposits of the Neogene Zagros basin Fatha, Injana, Mukdadiya, and Bai-Hasan Formations, as well as the Paleozoic Khabour, Pirispiki Formations and the Lower Cretaceous Garagu Formation (Fig. 2). Furthermore, five samples have been selected for detrital zircon (U-Th)/(He-Pb) double dating to tune-up the link between the source terrane exhumation and the hinterland deposition. The ultimate goal is to reconstruct provenance shifts in the erosional hinterland, which will build the bases to invoke the occurrence of specific geodynamic events throughout the Zagros orogeny including subduction, collision, and post-collisional thickening and uplift.

https://doi.org/10.5194/se-2021-68
Preprint. Discussion started: 19 May 2021


Solid Earth Discussions

2 Geologic background

2.1 The pre-Zagros orogeny strata

From the Cambrian and throughout most of the Paleozoic time (Fig. 2), the northeastern Arabian stratigraphic succession developed on the Pan-African basement and was part of the northern Gondwana along the Paleotethys Ocean. The Paleozoic stratigraphic column contains mostly clastic sedimentary rocks with some marginal marine carbonate successions (Konert et al., 2001). Prior to the onset of Variscan orogeny (Hercynian) during the late Devonian, the Arabian plate was considered as a stable platform. During the Variscan orogeny, however, the platform experienced intracratonic deformation, which lead to several zones of subsidence and uplift (Sharland et al., 2001). During the Permo-Triassic time, the eastern margin of Gondwana experienced a phase of rifting, and the Neotethys Ocean started to open. In the Kurdistan region of Iraq the exposed Paleozoic rocks includes two main clastic formations, which are referred to as the Khabour (Ordovician) and Pirispiki (Late Devonian) Formations (Al-Hadidy, 2007). The Khabour Formation consists of thin-bedded, fine-grained sandstones, quartzites, and shales that were deposited in a shallow to deep marine environment (van Bellen et al., 1959; Al-Bassam, 2010). The Pirispiki Formation includes sandstones, siltstones, and red mudstone beds, as well as conglomerates, which have been interpreted as records of a partially marine to a fluvial environment, but mostly non-marine (van Bellen et al., 1959; Al-Hadide et al., 2002; Al-Hadidy, 2007; Al-Juboury et al., 2020).

After the opening of the Neotethys Ocean during the Permo-Traissic, the border of the Arabian plate developed into a passive margin that accumulated thick sequences of limestones, shales, and evaporite beds during most of the Mesozoic (Fig. 2) (Sharland et al., 2001; Stampfli and Borel, 2002; Ziegler, 2001; English et al., 2015). During the Middle Jurassic, the Gotnia basin was formed, which hosted deep-water carbonates and shales that are currently encountered in Iraq (Aqrawi et al., 2010). During the late Jurassic, the west and northwestern part of Iraq experienced uplift, resulting in the formation of the Khlesia and Mosul basement highs, and the basin configuration changed considerably (Ameen, 1992; Aqrawi et al., 2010; English et al., 2015). This variation in basin geometry resulted in deposition of relatively thin (less than one hundred meter) carbonate rocks in association with clastic sandstone beds in the western side of the basin during the Early Cretaceous time. Toward the eastern side of the basin, a basinal carbonate succession such as the Balambo Formation (~2000 m) was deposited (van Bellen et al., 1959; Jassim and Buday, 2006; English et al., 2015). Later during most of the Late Cretaceous, the basin shallowed upward and filled with shelfal and lagaoonal carbonates that evolved from East to West. During the Campanian-Maastrichtian time, the northern Arabian plate was affected by a rifting phase that lead to the formation of grabens filled with synrift marly deposits. In addition, an environment with shallow water carbonates established on structural highs (Aqrawi et al., 2010; English et al., 2015).

2.2 The proto-Zagros foreland basin strata

By the Maastrichtian time the proto-Zagros flexural foreland basin started to form in response to arrival of the Neotethys intraoceanic subduction zone at the Arabia plate margin, leading to the ophiolite obduction (Homke et al., 2010; Saura et al., 2011; Barber et al., 2019). This process resulted in a basin geometry where the sedimentary infill thinned toward the West with a surge of clastic input sourced mostly from NW and NE (Karim and Surdashy, 2005; Aqrawi et al., 2010; Çelik and Salih, 2021). The main clastic formations of the proto-Zagros foreland basin in the Kurdistan region of Iraq are the Tanjero, Kolosh, and Gercus Formations with the ages of Maastrichtian, Paleocene, and Eocene respectively (Fig. 2) (van Bellen et al., 1959; Abdel-Kireem, 1986). The reported nature of the contact between these formations is both conformable and unconformable (van Bellen et al., 1959; Jassim and Sisakian, 1978; Tamar-Agha et al., 1978; Al-Shaibani and Al-Qayim, 1990; Jassim and Buday, 2006; Abdallah and Al-Dulaimi, 2019; Kharajiany et al., 2019). The depositional environment of the proto-Zagros foreland basin strata was interpreted as distal to proximal deep-marine deposits that shallows upward to a non-marine facies (Al-Qayim, 1994; Al-Qayim et al., 2008; Jassim and Buday, 2006; Kadem, 2006;

https://doi.org/10.5194/se-2021-68
Preprint. Discussion started: 19 May 2021

Al-Mashaikie et al., 2014). By the late Eocene, this clastic succession of the proto-Zagros foreland basis was covered by the shallow lagoonal marine carbonates of the Pila-Spi Formation (van Bellen et al., 1959; Aqrawi et al., 2010). The Pila-Spi Formations is then overlain by the lower/middle Miocene mixed clastic-carbonate-evaporite Fatha Formation following an unconformity during the Oligocene (Fig. 2) (Dunnington, 1958; Ameen, 2009; Lawa et al., 2013).

2.3 The Neogene Zagros Mesopotamia foreland basin strata

During the Neogene, the Arabia-Eurasia continent-continent collision became prominent and consequently new clastic material delivered into the newly flexural subsided basin (Fig. 2) (Koshnaw et al., 2017; 2020a). The synorogenic Neogene Zagros foreland basin formations are Fatha, Injana, Mukdadiya, and Bai-Hasan Formations. From bottom to top, the stratigraphic succession changes from the mixed clastic-carbonate-evaporite deposits of Fatha Formation to the meandering and braided fluvial, and alluvial deposits of the Injana, Mukdadiya, and Bai-Hasan Formations (Shawkat and Tucker, 1978; Tamar-Agha and Al-Aslami, 2015; Tamar-Agha and Salman, 2015; Koshnaw et al., 2020a).

2.4 The Red Beds Series strata

The Red Beds Series (RBS) is located along the suture zone in the hinterland of the northwestern Zagros fold-thrust belt on the Arabian plate and overthrust by the Main Zagros fault (Fig. 1b). The RBS deposits consist of several NW-SE oriented discrete outcrops where alternating mudstones, sandstones, conglomerate beds, as well as carbonate beds are encountered. They have been grouped into three major units: Suwais Group, Govanda Formation, and Merga Group. The Suwais and Merga Groups have been further subdivided into four and two subgroups respectively based on their lithofacies. Generally, the thickness of the clastic Suwais Group varies geographically between 1000 - 1500 m. In some locations, this unit is even thicker. Overall, the Suwais Group represents a succession of dark red mudstone, siltstone, and sandstone with frequently occurring conglomeratic beds. Generally, the suite coarsens and thickens upward so that the conglomerate beds with cobbles and boulders become the dominant lithofacies towards the upper part. The Suwais Group is regarded as marine to mostly non-marine fluvial deposits (Jassim et al., 2006; Alsultan and Gayara, 2016). A Paleocene-Eocene depositional age has been inferred for this unit based on fossil contents, for which, however no list has been reported (Jassim et al., 2006), Recently, using detrital zircon ages as criteria, Koshnaw et al., (2019) inferred a maximum depositional age as old as the late Oligocene (~26 Ma).

The Suwais Group conformably overlies the Maastrichtian Tanjero Formation, but it was considered to follow the Lower Cretaceous Qulqula Formation with an unconformity (Karim et al., 2011; Hassan et al., 2014). However, using the late Oligocene maximum depositional age of the Suwais Group as criteria, Koshnaw et al. (2019) interpreted that the contact with the Tanjero Formation as unconformable. The upper contact of the Suwais Group with the Govanda Formation is reported as unconformable (Jassim et al., 2006). The Govanda Formation comprises ~100-120 m-thick reefal limestones with a few sandstone and conglomerate interebeds. Based on fossiliferous records, a Burdigalian to Langhian depositional age was proposed (van Bellen et al., 1959; Abdula et al., 2018). The ~200-500 m-thick Merga unit, which overlies the Govanda Formation (Fig. 2), consists of red mudstones and sandstones, some conglomerate interbeds with cobbles and boulders particularly in the upper ~200 m of the Merga Group. This group is considered to have been deposited in a fluvial to alluvial environment (Jassim et al., 2006; Alsultan and Gayara, 2016). The contact between the Govanda Formation and Merga Group is conformable (van Bellen et al., 1959; Jassim et al., 2006).

3 Structural and stratigraphic relationships with the Red Beds Series

In the northwestern Zagros suture zone the RBS series are overthrusted by the Qandeel Series, Walash Group, and Naopurdan Group (Fig. 3). Along strike, these units are interchangeably thrust onto the Red Beds Series and they mark the

https://doi.org/10.5194/se-2021-68
Preprint. Discussion started: 19 May 2021

Main Zagros fault (Fig. 1b). In the vicinity of the Main Zagros fault, angular unconformities are preserved between the older Upper Cretaceous formations and (i) the middle Miocene Govanda Formation on the northwestern plunge, and (ii) the upper Oligocene – lower Miocene (?) Suwais Group on the southeastern plunge of the Tanun anticline (Figs. 4 and 5). Along strike farther to the southeast, an angular unconformity between the Red Beds Series (Suwais Group) and the Lower Cretaceous Qulqula radiolarites is also preserved (Karim et al., 2011). Structurally, the highest unit is the Qandeel Series, which is an ophiolite-bearing Upper Cretaceous metamorphosed klippe that likely disjointed by an out-of-sequence deformation from the adjacent terranes of the Sanandaj-Sirjan zone (SSZ) (Jassim et al., 2006; Ali et al., 2014; Ali et al., 2019). The Walash Group (Fig. 6a,b), below the Qandeel Series thrust sheet, is a volcaniclastic unit that made up of dark red mudstones, shales, slates, relatively limited beds of sandstone and conglomerates, radiolarites and limestone beds, and metasediments near the top. These beds are associated with pyroclasts, basic pillow lava (diabase, pyroxene-bearing spilitic basalt, and spilite) and basaltic andesite flow (pyroxene andesite and amphibole andesite), (Jassim et al., 2006; Ali et al., 2013). Pyroclastic feldspar of the Walash Group has been dated by the $^{40}Ar/^{36}Ar$ method and yielded 43.01 ± 0.15 Ma (Ali et al., 2013). Additionally, the $^{40}Ar/^{36}Ar$ age of the andesite lava flow is 43.1 ± 0.3 Ma, and the diabase rock is 40.1 ± 0.3 – 32.3 ± 0.4 Ma (Aswad et al., 2014). The isochronal age of $^{87}Rb/^{86}Sr$ yielded ~44 Ma (Koyi, 2009). Depending on the planktonic and benthic foraminiferal assemblages, a marine environment with a depositional age of middle Eocene (Lutetian) has been proposed (Al-Banna and Al-Mutwali, 2008). The Walash Group itself thrusts onto the Naopurdan Group, which is mostly made up of metasedimentary rock, but includes basalt flow and pillow lavas as well. The Naopurdan Group (Fig. 6c,d,e) is composed of sandstones, shales, and conglomerates with basic volcanic, nummulitic limestone slate constituents. The upper part consists of an upward coarsening succession from sandstones to conglomerates with basic volcanic clasts (Jassim et al., 2006; Ali et al., 2013). Based on the planktonic foraminiferal assemblage, a marine environment of Eocene age has been suggested (Jassim et al., 2006), but $^{40}Ar/^{36}Ar$ ages measured on basaltic feldspars yielded younger ages between 24.31 ± 0.60 Ma and 33.42 ± 0.44 Ma and (Ali et al., 2013). The Naopurdan Group thrusts onto the autochthonous Red Beds Series deposits (Suwais Group, Fig. 6g, Govanda Formation, and Merga Group, Fig. 6h) on the Arabian plate. Along the thrust, the Naopurdan Group shows clear evidence for tectonic deformation such as slate pencil cleavage (Fig. 4e). At a different locality below the Naopurdan thrust sheet, the Merga Group shows a well-developed shear zone with c- and s-planes (Fig. 6f).

4 Detrital zircon geochronology and thermochroology

4.1 Sampling and methods

In this paper 1097 new detrital zircon U-Pb ages and 74 new detrital zircon (U-Th)/He ages are presented, from eight samples from the Red Bed Series and three samples from the proto-Zagros formations. These new data are integrated with previously published U-Pb age results in the study area (Koshnaw et al., 2019; Koshnaw et al., 2020a). Additionally, five samples from the Red Bed Series were chosen for the detrital zircon (U-Th)/(He-Pb) double dating.

All sample preparation and analyses on the new samples were conducted at the University of Texas at Austin Geo- and Thermochronometry and mineral separation laboratories. Mineral separation was conducted following mineral separation procedure (e.g., Gehrels, 2000) and ~120 zircon grains of different size (30–100 μm) and shape were selected randomly for the analysis from each sample. The zircon U-Pb ages were produced using the Laser Ablation Inductively Coupled Plasma Mass Spectrometry (LA-ICP-MS) following procedures outlined in Marsh and Stockli (2015) and Hart et al. (2016). In order to preserve the zircon grains for future (U-Th)/He analyses, the detrital zircon geochronologic ages were obtained by depth-profile U-Pb analysis on unpolished grains (Stockli, 2017). The reported zircon U-Pb ages in this study represent discordance ages <20 % with 2σ analytical uncertainty. The age concordance was determined based on the age of

https://doi.org/10.5194/se-2021-68
Preprint. Discussion started: 19 May 2021

$^{206}Pb/^{238}U$ for zircon grains <950 Ma, and the $^{207}Pb/^{206}Pb$ age for grains >950 Ma. After completion of the U-Pb analytical process, 13-21 representative zircon grains (except sample 12KRD-132, n=7) from major age peaks were manually picked from the tape mount and packed in a platinum (Pt) pocket for zircon (U-Th)/He thermochronometric analysis. The presented zircon helium ages in this study are alpha ejection corrected (Farley et al., 1996) with standard procedure uncertainty of ~8% and 2σ (Reiners et al., 2002). The zircon (U-Th)/He ages were acquired following the methodology described in Wolfe and Stockli (2010). For detailed laboratory and data reduction processes please refer to Thomson et al. (2017), Xu et al. (2017), and Pujols et al. (2020).

4.2 Detrital zircon U-Pb geochronology results

The detrital zircon U-Pb age distributions from three new proto-Zagros foreland basin samples manifest a unimodal U-Pb age spectra of Early-Late Cretaceous time (~120-85 Ma) throughout the Tanjero (12KRD-142: ~120-90), Kolosh (12KRD-143: ~105-85), and Gercus (12KRD-146: ~110-85) Formations, with an age peak of ~100 Ma (Fig. 7b). Among these, the Kolosh sample 12KRD-143 contains relatively two young grains of middle Eocene (~40 Ma). Interestingly, the detrital zircon U-Pb age populations that are determined for the Upper Cretaceous-Eocene proto-Zagros foreland basin fill are very different compared to the older Paleozoic and Lower Cretaceous pre-Zagros deposits and the younger Neogene Zagros foreland fill (Fig. 7a,c) (Koshnaw et al., 2020a). The new detrital zircon U-Pb age results from the eight Red Beds Series samples display a bimodal signature with the late Eocene (~35-45 Ma) and Paleocene (~55-65 Ma) ages with peaks of ~40 Ma and ~60 Ma (Fig. 8). Less commonly an older age peak of ~100 Ma is also found, except a samples from the Suwais Group (SH17S2) that shows a dominant ~100 Ma peak.

4.3 Detrital zircon (U-Th)/He thermochronology and (U-Th)/(He-Pb) double dating results

To further constrain the potential source regions for the Red Beds Series deposits, five samples were chosen for zircon (U-Th)/He thermochronometric analysis (ZHe) and (U-Th)/(He-Pb) double dating. Two samples were collected from the NW area and three specimens from SE area, including the Suwais and Merga Groups in each area (Fig. 9). Detrital zircon grains were selected from each main U-Pb age peaks including: ~40 Ma (late Eocene), ~60 Ma (middle Paleocene), ~75 Ma (Late Cretaceous), ~100 Ma (late Early Cretaceous), ~170 Ma (Jurassic), ~300 Ma (Carboniferous-Permian), ~600 Ma (Neoproterozoic). Generally, the bulk ZHe age results display notable ranges of ~66-55 Ma with a peak age of ~60, and ~50-35 Ma with peaks of ~40 Ma for the Suwais Group, and ~45 and ~37 Ma for the Merga Group (Fig. 9a). Two grains from the Merga Group that are extracted from the samples MT17M3 and SH17M5, chronicle the youngest exhumation at ~21 Ma. From the Suwais Group, three ZHe ages that overlap within error mark the youngest peak of ~29 Ma. The detrital zircon (U-Th)/(He-Pb) double dating results reveal cooling ages of ~40-30 Ma for the late Eocene grains and ~60-40 Ma for the middle Paleocene grains (Fig. 9b,c). The Late and late Early Cretaceous zircon grains have cooling ages of ~70-35 Ma. The Jurassic zircon grains show cooling ages of ~60-40 Ma, comparable to the middle Paleocene zircon grains. The Neoproterozoic and Carboniferous-Permian zircon grains manifest a wide range of cooling ages of ~150-30 Ma and ~120-50 Ma, respectively.

5 DISCUSSION

5.1 Sedimentary provenance evolution

5.1.1 Provenance of the NW Zagros wedge-top deposits

The new detrital zircon U-Pb age results form this study highlight distinctive signatures for each of the various tectonic phases including: (i) the passive margin pre-Zagros orogeny, the proto-Zagros foreland basin stage related to the

https://doi.org/10.5194/se-2021-68
Preprint. Discussion started: 19 May 2021

obduction of the oceanic crust, and (iii) the post continental collision-related Neogene Zagros basins (Fig. 10a,b). In particular, the provenance data from the Tanjero, Kolosh, and Gercus Formations, from the proto-Zagros foreland basin, show a strong influence of Neotethys-related terranes and a striking difference with the older and younger formations, implying a switch of the main sediment sources through time. The key source terranes in the NW Zagros and the surrounding areas are (i) the Paleocene-Eocene Walash-Naopurdan-Kamyaran complex (WNK), (ii) the Cretaceous Neotethys oceanic crust and the island arc ophiolitic terranes, (iii) the Jurassic and Triassic igneous rocks within the Sanandaj-Sirjan zone (SSZ), (iv) the Carboniferous-Permian Variscan rocks, and (v) the Neoproterozoic Pan-African/Arabian-Nubian shield and older rocks.

Samples from the proto-Zagros foreland basin formations that were obtained from the NW of the study area (Fig. 1b) have a sole age peak of ~100 Ma. This age peak points at the Neotethys oceanic crust and island arc ophiolitic terranes as the principal source during the Maastrichtian and the Paleogene times in the NW of the proto-Zagros foreland basin. The older pre-Zagros passive margin strata (Paleozoic and Lower Cretaceous) form the northern part of the study area (Al-Juboury et al., 2020; Koshnaw et al., 2020a), unlike the proto-Zagros formations, have detrital zircon U-Pb age distributions dominated by older sources such as Early Neoproterozoic, Pan-African, Cadomian (peri-Gondwana), and other Gondwana-related sources (Fig. 7). These age components are also found in the detrital zircon populations of the Lower Cretaceous formations in the southern Iraq (Wells et al., 2017). The sediment of the Paleozoic and Lower Cretaceous rocks are largely originated from the Arabian-Nubian shield, the Gondwana super-fan system, and the Cadomian terranes (Avigad et al., 2016, 2017; Koshnaw et al., 2017; Meinhold et al., 2021). This contrast in provenance signature between the pre-Zagros and proto-Zagros deposits reflect a fundamental reversal in the sediment routing system from the West to the East as the basin started to flex due to arrival of the Neotethys ophiolitic island arc and oceanic curst terranes that are associated with numerous Upper Cretaceous intrusions (Delaloye and Desmons, 1980; Ali et al., 2012; Nouri et al., 2016; Al Humadi et al., 2019; Ismail et al., 2020). However along-strike toward SE, the proto-Zagros strata of the Amiran and Kashghan Formations have a ~240 Ma Triassic age mid-oceanic ridge signature (Zhang et al., 2016; Barber et al., 2019) in addition to the ~100 Ma signature, implying a different paleogeography toward NW. As zircon in mafic rocks is not a common mineral (Grimes et al., 2007), sandstone petrographic analysis on the Tanjero Formation revealed contents of limestone and chert (Aziz and Sadiq, 2020; Jones et al., 2020) that were particularly sourced from the older Qulqula radiolarite and Balambo Formations in the NW (Çelik and Salih, 2021). Such variation in the sediment source for the proto-Zagros foreland basin is in line with the destruction of the Gotnia basin architecture and the recycling of its deposits into the newly flexural basin and the occurrence of some Paleozoic and older zircon grains in the Tanjero Formation (Aqrawi et al., 2010; English et al., 2015; Aziz and Sadiq, 2020; Jones et al., 2020). The younger Neogene Zagros foreland basin strata have also distinct U-Pb age spectra dissimilar to the proto-Zagros and pre-Zagros U-Pb age distributions. In the same locality where the new proto-Zagros samples were obtained, published data show that most of the Neogene formations, except the Injana Formation, are dominated by characterized by an Eocene (~40 Ma) peak with subordinate contributions of older ages. However, in different localities, the Neogene deposits show a more mixed signature. These deposits were interpreted to have been delivered by transverse rivers from NE and during the late stage of the Zagros orogeny (Koshnaw et al., 2020a). Together with the Eocene peak in the U-Pb age detrital zircon ages (~40 Ma), the Injana Formation records a wider range of source terranes with a younger early Oligocene ages and older age components that were likely recycled from older uplifted strata and delivered by axial rivers from the NW (Koshnaw et al., 2020a).

Ultimately, such variation in the detrital zircon U-Pb provenance between the different hinterland wedge-top units of the Zagros basin denote that (i) the pre-Zagros passive margin deposits are diagnosed by a wide age range of old zircon grains, (ii) the proto-Zagros Neotethyan terrane obduction-related deposits record unique Albian-Cenomanian aged zircon grains, and that (iii) the Neogene Zagros foreland basin deposits contain zircon grains with Eocene and early Oligocene U-Pb ages.

https://doi.org/10.5194/se-2021-68
Preprint. Discussion started: 19 May 2021

5.1.2 Provenance of the NW Zagros Red Beds Series deposits

The Red Beds Series (RBS) provenance data puts an age limit on the along-strike diminution of the magmatic activities and on the exhumation of the source terranes. The detrital zircon U-Pb age populations from the Red Beds Series depict two key components which are Paleocene ages with a peak of ~60 Ma, and late Eocene ages with a peak of ~40 Ma (Fig. 8). Zircon grains from these two age components record identical (U-Th)/He and U-Pb ages, pointing towards a volcanic origin (Fig. 9b,c). Furthermore, their cooling over ~60-40 Ma for the middle Paleocene grains and ~40-30 Ma for the late Eocene grains suggest systematic exhumation and unroofing of magmatic plutons through time. In the vicinity of the Red Beds Series, the potential source terrane candidates that have comparable ages are the Walash-Naopurdan volcaniclastic complex and Urumieh-Dokhtar magmatic zone (UDMZ), which both are located to the NE of the study area.

The Paleogene Walash-Naopurdan volcaniclastic complex extends along-strike into Iran and was previously termed as Walash-Naopurdan-Kamyaran (WNK) (Ali et al., 2014; Moghadam et al., 2020). The Walash-Naopurdan complex is equivalent to the volcaniclastic deposits near Kamyaran and Kermanshah in Iran, which have been named differently as Gaveh-Rud domain (Braud and Ricou, 1975; Homke et al., 2010; Saura et al., 2015), Early Tertiary magmatic domain (Agard et al., 2005, 2011), and Kamyaran Paleocene-Eocene arc (Whitechurch et al., 2013). These Paleogene rocks represent arc-related (defined differently as arc, backarc, and forearc) volcanic and volcaniclastic units (Homke et al., 2010; Ali et al., 2013; Whitechurch et al., 2013; Saura et al., 2015), which likely developed in the proximity of the southwestern margin of the Eurasian plate in association with the subduction of the Neotethys plate beneath Eurasia (Homke et al., 2010; Agard et al., 2011; Whitechurch et al., 2013; Saura et al., 2015). The dated magmatic bedrocks within the WNK complex and part of the adjacent Sanandaj-Sirjan-Zone (SSZ) show both age components that are found in the RBS, i.e., Paleocene (Braud, 1987 in Homke et al., 2010; Azizi et al., 2011; Whitechurch et al., 2013) and Eocene (Mazhari et al., 2009, 2020; Azizi et al., 2011, 2019; Ali et al., 2013; Aswad et al., 2014; Moghadam et al., 2020). The Eocene age intrusions are also found within the Late Cretaceous ophiolitic rocks (Leterrier, 1985; Aswad et al., 2016; Ali et al., 2017; Ismail et al., 2020). Younger Oligocene magmatic rocks within the WNK complex have also been reported (Whitechurch et al., 2013; Ali et al., 2013). The UDMZ (Urumieh-Dokhtar magmatic zone), which is an Andean-type continental arc zone, contains large Eocene and Oligocene igneous bodies marking a prolonged magmatic flare-up (Verdel et al., 2011; Chiu et al., 2013) with a peak magmatism age of ~40 Ma (van der Boon et al., 2021). Accordingly, both the WNK and the UDMZ could have served as source areas for the Red Bed Series. However, the WNK complex is thrusted onto the RBS and it is adjacent to the SSZ, whereas the SSZ is situated between the RBS and the UDMZ, which makes any sedimentary pathways more complicated. In addition, the recorded RBS detrital zircon exhumation timing of ~60-40 Ma and ~40-30 Ma are contemporaneous with the ~60-40 Ma exhumation timing of the SSZ on the basis of (U-Th)/He ages of the Jurassic zircon grains. Because the regional uplift of the SSZ occurred earlier than that of the UDMZ, it is very unlikely that large volumes of UDMZ material were supplied to the Red Bed Series depocenter since uplift of the SSZ disconnected the sedimentary pathways (François et al., 2014; Barber et al., 2018).

The new and published data of the RBS collectively illustrate that the youngest zircon age peak of the Suwais Group samples is between ~37 Ma and ~41 Ma. In the same sense, the youngest zircon age peak of the Merga Group samples is between ~36 Ma and ~45 Ma, however a younger ~33 Ma peak (three grains) also exists (Fig. 8). Along-strike, both groups show older ages toward SE, similar to the age trend of the Walash and Naopurdan rocks, ~24-33 Ma in the NW and ~32-43 Ma in the SE (Ali et al., 2019).

So far in the vicinity of the study area, the late Oligocene magmatism has been documented only in two localities in the northwestern Zagros, including the Kurdistan region of Iraq and Iran (Ali et al., 2013; Whitechurch et al., 2013), but further NW in Iran magmatism is more abundant (Agard et al., 2011; Chiu et al., 2013). In general, magmatic activity appears to be considerably less during the late Oligocene than during the Eocene (van deer Boon et al., 2021). In the Kurdistan region of Iraq, earlier partial cessation of magmatism in the southeastern part is potentially due to presence of the

https://doi.org/10.5194/se-2021-68
Preprint. Discussion started: 19 May 2021

Bisotoun block (Agard et al, 2005, Wrobel-Daveau et al., 2010; Sasvari et al., 2015), which implies that the thrusting of the WNK terranes occurred earlier in the SE of the study area. As the geographic extension of the of the Bisotoun block is limited, this local difference in the timing of the WNK terrane thrusting can not be in contradiction with the regional oblique Arabia-Eurasia collision that likely commenced first farther in the NW, away from the study area (e.g. Rolland et al., 2011; Darin et al., 2018).

Overall, the U-Pb age populations of the Red Beds Series deposits show consistent detrital zircon age signatures from the bottom to the top, which imply that the WNK complex was the major source area, and that the sediment sources have not changed during deposition of the RBS.

5.2 Basin dynamic of the NW Zagros Red Beds Series deposits

The angular unconformity between the Suwais Group and the Upper Cretaceous strata, and the detrital zircon U-Pb and (U-Th)/(He-Pb) double dating results advocate for a deposition of the RBS in a distinctive hinterland basin.

On the basis of the documented growth strata in the Masstrichtian Tanjero Formation of the Tanun anticline (Le Garzic et al., 2019) and the lack of growth strata in the Suwais Group (Fig. 5c), the Suwais Group deposition must have been taken place after the deposition of the Tanjero Formation and the initial growth of the Tanun anticline. This period of non-deposition is also evident from the ~26 Ma detrital zircon maximum depositional age of the Suwais Group (Koshnaw et al., 2019) and the Masstrichtian age of the Tanjero Formation (Abdel-Kireem, 1986). However, no direct angularity is manifested between the Tanjero Formation and the Suwais Group (Le Garzic et al., 2019), possibly because of erosion of the tilted beds of the Tanjero Formation where the Suwais Group is deposited and the preservation of the semi-horizontal beds. This angular unconformity between the Suwais Group and the Upper Cretaceous beds along with other angular unconformities between the Suwais Group and the Qulqula Formation (Karim et al., 2011), the Govanda Formation and the Upper the Cretaceous beds suggest the occurrence of deposition in an intermontane setting after the development the proto-Zagros fold-thrust belt (Lawa et al., 2013; Koshnaw et al., 2017, 2020a; Le Garzic et al., 2019).

The comparison of the RBS, pre-Zagros, proto-Zagros, and Neogene Zagros detrital zircon U-Pb provenance data reveals a robust dissimilarity of the RBS deposits with pre-Zagros and proto-Zagros units, but possible a linkage with the Neogene Zagros units (Fig. 10). Additionally, the sandstone petrography shows that both the Suwais Group and the Tanjero Formation are litharenites, yet a key difference is the presence of the magmatic and metamorphic grains in the Suwais Group and their lack in the Tanjero Formation (Hassan et al., 2014; Çelik and Salih, 2018, 2021)

To further constrain the tectonic setting of the RBS, three principal hypotheses can be tested: (a) RBS deposited in a foreland basin; (b) RBS deposited in a foreland basin, but later developed into an intermontane basin; (c) and RBS deposited in an intermontane basin (Fig. 11). To render a unique solution, detrital zircon (U-Th)/(He-Pb) double dating method has been utilized. In scenario a, as the proto-Zagros foreland basin detrital zircon spectra is a dominated by a ~100 age peak (this study) and characterized by a ~70 Ma peak exhumation age (Barber et al., 2019), the RBS deposits are expected to have a similar signature. In scenario b, because the RBS deposition involves an early stage foreland and a late stage intermontane basin a mixed U-Pb age distribution from the recycled ~100 Ma grains with a ~75 Ma ZHe age and new ~60 Ma and ~40 Ma grains with their corresponding ZHe ages are expected. In scenario c, as the RBS tectonic setting is unrelated to the foreland basin, a mixed U-Pb age spectra similar to the scenario b is predicted, yet with no inherited ~75 Ma ZHe age because no recycling of foreland basin strata is expected. The scenario a can be ruled out as the RBS detrital zircon U-Pb age spectra is predominantly different (Figs. 7,8, and 10). Scenario b and c can be proportional, but there are two key differences in the U-Pb and (U-Th)/He ages. In scenario b, because the RBS basin involves an early stage foreland basin, no detrital zircons with a Paleocene and Eocene age should be expected from its lower strata. However, samples from the Suwais Group are dominated by the Paleocene and Eocene age components (Fig. 8). Additionally, the detrital zircon (U-Th)/(He-Pb) double dating results (Fig. 9) show that most of the ~100 Ma U-Pb age grains have a similar exhumation age to the Paleocene and

https://doi.org/10.5194/se-2021-68
Preprint. Discussion started: 19 May 2021

Eocene age grains and cluster around ~65 Ma and ~40 Ma. These ages are till younger than the ~70 Ma ZHe exhumation age of the proto-Zagros strata. Moreover, due to presence of the ~40 Ma ZHe ages and insufficient burial in the proto-Zagros basin to reset ZHe ages, the ~100 Ma U-Pb ages are unlikely a signal recording an origin from the deformed proto-Zagros strata but rather from newly eroded ophiolitic terranes with similar igneous intrusions. The pre-deformational thickness of the proto-Zagros formations collectively (Tanjero, Kolosh, Gercus Formations) is about 3-3.6 km (van Bellen et al., 1959). Assuming 20^{o} for the surface temperature and 25^{o} C/km for the geothermal gradient, about 6-7 km thickness would be required to reset ZHe ages. Therefore, on the basis of the detrital zircon U-Pb signature and the (U-Th)/(He-Pb) double dating results, we argue that scenario c, the intermontane basin hypothesis, is more plausible and compatible with the provenance characteristics of the RBS deposits.

All-inclusive, the angular unconformities and the provenance information suggest no connection of the RBS intermontane basin with the proto-Zagros foreland basin and limited connection with the Neogene Zagros foreland basin, possibly as a result of the broader Zagros collisional zone uplift and exhumation at a late stage.

5.3 Geodynamic evolution

The new field evidence and provenance data and interpretation from this study along with the existing knowledge about the magmatic and tectonic history of the Arabian and Eurasian margins unravel the Cenozoic convergence history between the two plates (Figs. 12 and 13)

After the initiation of the Neotethys interoceanic subduction zone during the Aptian, its development until the middle Late Cretaceous, including the growth of ophiolitic island arcs (Aswad and Elias, 1988; Aziz et al., 2011; Ali et al., 2012; Barber et al., 2019), the ophiolitic terranes obducted on the northeastern margin of Arabian plate during the Campanian (Fig. 13a) and shed sediments on the newly formed proto-Zagros foreland basin as evidenced from the detrital zircon provenance from this study and the detrital zircon ZHe from the Amiran and Kashghan Formations from Lurestan in Iran (Barber et al., 2019). In the Upper Cretaceous Bekhma Formation (late Campanian-early Maastrichtian age; van Bellen et al., 1959) the U-Pb dating of hydrothermal cementation yielded ~74 Ma (Salih et al., 2019), consistent with the detrital geochronological and thermochronological constrains. These lines of evidence suggest that the proto-Zagros fold-thrust belt growth initiated as a result of the ophiolite obduction.

During the Paleocene and Eocene (Fig. 13b,c), significant tectonomagmatic events took place along the Arabian and Eurasian plates. During the Paleocene (Fig. 13b), the WNK complex possibly originated as a back-arc to arc system, associated with magmatic activity (Braud, 1987 in Homke et al., 2010; Azizi et al., 2011, 2019; Ali et al., 2013; Whitechurch et al., 2013). The signature of the Paleocene magmatism is also reflected in the detrital zircon U-Pb and (U-Th)/He record of the Red Beds Series that derived from the WNK complex. The locality of this arc system is contested as it is not clear whether it developed in the vicinity of the Eurasian plate (Agard et al., 2005; 2011; Al-Qayim et al., 2012; Whitechurch et al., 2013) or close to the Arabian plate (Aswad et al., 2014; Ali et al., 2017, 2019). However, due to presence of Eurasian derived detritus (Homke et al., 2010; Whitechurch et al., 2013) and the occurrence of low-grade metamorphic grains (Ali et al., 2017), which are abundant in the Sanandaj-Sirjan zone (SSZ) (Hassanzadeh and Vernicke, 2016), a Eurasian-related setting that resulted from the oceanic slab rollback is more likely (Whitechurch et al., 2013). During the Eocene (Fig. 13c), the magmatism in the WNK complex and SSZ edge continued (Mazhari et al., 2009, 2020; Azizi et al., 2011, 2019; Ali et al., 2013; Whitechurch et al., 2013; Aswad et al., 2014; Moghadam et al., 2020). This period of magmatism in the WNK complex was coeval with the nearby voluminous UDMZ magmatic flare-up (Verdel et al., 2011; Chiu et al., 2013; van der Boon et al., 2021), implying a genetic relationship. The downgoing oceanic slab was possibly sunk deeper and further beneath the Eurasian plate with a relatively shallower angle that led to the generation of magmas in the WNK and UDMZ at a comparable period (Whitechurch et al., 2013; Hassanzadeh and Vernicke, 2016). Additionally, the Cretaceous ophiolitic units are also containing Eocene intrusions (Leterrier, 1985; Aswad et al., 2016; Ali et al., 2017; Ismail et al., 2020), with an

https://doi.org/10.5194/se-2021-68
Preprint. Discussion started: 19 May 2021

origin that was most likely different to that of the WNK complex (Aswad et al., 2016). These Eocene intrusions in the Cretaceous ophiolitic terranes are likely the consequence of the downgoing oceanic slab breakoff in the proximity of the Arabian plate. Tomographic images for the Middle East show a deeply sunken cold material that has been considered as a remnant from an older early Paleogene slab breakoff event. This inferred cold material is different from the remnant of a younger (Miocene) and shallower slab breakoff (Mesopotamia and Zagros slabs; van der Meer et al., 2018).

For this period, the Eocene, several models suggested multiple subduction zones with 200-300 km distance between the zones across the Neotethys to explain the documented magmatic activities (Aswad et al., 2016; Ali et al., 2017; Ali et al., 2019). However, due to space problems and difficulties of subduction inception a multiple subduction system has been considered as unlikely (Whitechurch et al., 2013). Present-day natural examples of a single complete suite of trench, forearc, arc, back-arc necessitate 200-500 km horizontal width, depending on the subduction angle (Cloos et al, 1993; Stern, 2002, 2010). By utilizing plate kinematic reconstruction software (Gplates 2.2.0, Müller et al., 2018), based on the plate circuit model of Arabia-Eurasia (McQuarrie and Hinsbergen, 2013), at ~40 Ma the calculated distance between the Arabian and Eurasian margins is estimated to be 283 ± 66 km. For this calculation the length of the Harsin (35 km) and Bisotun (49 km) domains were excluded (Vergés et al., 2011), as the study area is farther NW of Lurestan and no evidence has been found regarding their presence. Therefore, we hypothesize that the 283 ± 66 km distance between the Arabian and Eurasian plates is more compatible with a convergence model that involves a subduction of the Neotethys slab below Eurasia, and older subducted slab below the obducted ophiolite on Arabia.

The late Eocene to the late Oligocene (~36-26 Ma) marks a period of significant reduction of magmatism in the UDMZ, WNK complex, and in the Late Cretaceous ophiolitic terranes. During the same time, widespread unconformity has been recorded (Dunnington, 1958; Ameen, 2009; Lawa et al., 2013). Furthermore, development of syndepositional compressional shear joints within the upper Eocene Pila-Spi Formation has also been documented (Numan et al., 1998) in the Zagros fold-thrust belt. Lastly, fractures that filled by hydrothermal cementation in the in the Zagros fold-thrust belt hint at a period of fluid flow during the early Oligocene (~30 Ma), an age constrained by U-Pb method (Salih et al., 2019). Among the presented RBS samples, there are four young detrital zircon age peaks of ~36-37 Ma (Fig. 8). Such detrital zircon pattern signifies a remarkable attenuation of magmatism in the source terranes by ~36 Ma. However, the occurrence of a single younger peak of ~33 Ma, and limited younger magmatic activity of ~26 Ma (Whitechurch et al., 2013) and ~24 Ma (Ali et al., 2013) imply that magmatic activities continued locally. Samples from the RBS, particularly from the bottom section of the Suwais Group (e.g. sample CH17S10, Fig. 5c), which includes an Eurasian signature, contain a zircon grain as young as ~26 Ma (Koshnaw et al., 2019). We argue that these data brackets the Arabia-Eurasia collision between ~36 Ma and ~26 Ma from the commencement to the termination in the northwestern Zagros, a conclusion in agreement with previous studies (Hempton, 1987; Agard et al., 2005, 2011; Horton et al., 2008; Mark and Armstrong, 2008; Ballato et al., 2011; Mouthereau et al., 2012; Barber et al., 2018).

After the continental collision, the Zagros suture, as well as the SSZ and the UDMZ underwent notable uplift and exhumation starting the earliest Miocene (Figs. 12 and 13e). The youngest detrital zircon grains from the RBS deposits (Merga Group) record a ~21 Ma ZHe exhumation age, comparable to (i) the ~23 Ma ZHe age of an Eocene intrusion within the Cretaceous ophiolite (Ismail et al., 2020), (ii) the period of accelerated exhumation in the SSZ and UDMZ as documented by apatite (U-Th)/He (AHe), apatite fission track (AFT), and zircon fission track (ZFT) ages (François et al., 2014; Behyari et al., 2017; Barber et al., 2018), and (iii) a ~22 Ma AFT detrital age from the Aghajari Formation of the Neogene Zagros foreland basin in Lurestan in Iran (Homke et al., 2010). Additionally, the earliest Miocene is also the time of alkaline magmatism initiation in the UDMZ (Homke et al., 2010 and references therein; Mouthereau et al., 2012 and references therein; van der Boon, 2021). Furthermore, the present-day field relationship reveal that in some localities the Cretaceous ophiolitic terranes, including the associated Eocene intrusions that have different petrochemistry than the Eocene WNK, were thrust onto the WNK (e.g. Figs. 4 and 5a) likely as an out-of-sequence mechanism (Ali et al., 2014; Aswad et

https://doi.org/10.5194/se-2021-68
Preprint. Discussion started: 19 May 2021

al., 2016). Such event likely occurred at a similar time to the documented ~21-23 Ma exhumation age across the Zagros broader collisional zone as a consequence of the terminal collision. Later, further enhanced exhumation took place during the middle and late Miocene (~14-4 Ma) from the suture zone forelandward with sediment inputs from the NW and NE of the study area, which possibly triggered by a new slab breakoff event (Koshnaw et al., 2020a,b).

5 Conclusions

Angular unconformity between the Red Beds Series (RBS) units, the Suwais Group and the Govanda Formation, and the deformed Upper Cretaceous formations in the NW Zagros hinterland denotes deposition of the RBS in an intermontane basin after the proto-Zagros fold-thrust belt development. The detrital zircon U-Pb data of the RBS units (Suwais and Merga Groups) and the proto-Zagros foreland basin strata (Tanjero, Kolosh, and Gercus Formations) are strikingly different, yet they are partially commensurate with the Neogene Zagros foreland basin fill, and all data sets are unrelated to the pre-Zagros Paleozoic and Lower Cretaceous record. The detrital zircon (U-Th)/(He-Pb) double dating result pattern of the RBS further highlight an intermontane basin setting and demonstrate volcanic input and unroofing of potential plutons, dissimilar to the proto-Zagros detrital record. Provenance evaluation shows derivation of the RBS deposits form the Paleogene Walash-Naopurdan-Kamyaran arc-related complex that was developed along Eurasian margin, whereas the proto-Zagros deposits from the Late Cretaceous ophiolitic terranes. Cutback of magmatism significantly in the source regions by ~36 Ma as reflected in the RBS youngest U-Pb age peaks points at the late Eocene time as the onset of the Arabia-Eurasia collision in the NW Zagros. Altogether, the provenance shift of the pre-Zagros, proto-Zagros, and Neogene Zagros units, reduction of magmatism, deposition of the WNK-derived RBS in an intermontane basin reflect different phases of the Cenozoic Zagros orogeny.

Acknowledgments

This research was partially funded by the State Secretariat for Education, Research and Innovation of Switzerland via the Swiss Government Excellence Scholarship awarded to R. Koshnaw. We thank I. Ahmed, V. Sissakian, M. Tamar-Agha, W. Shingaly, N. Karo, M. Zebari for discussion and logistical support. We extend gratitude to R. Chatterjee, D. Patterson, and L. Stockli at the University of Texas at Austin UTChron laboratories for their assistance.

https://doi.org/10.5194/se-2021-68
Preprint. Discussion started: 19 May 2021

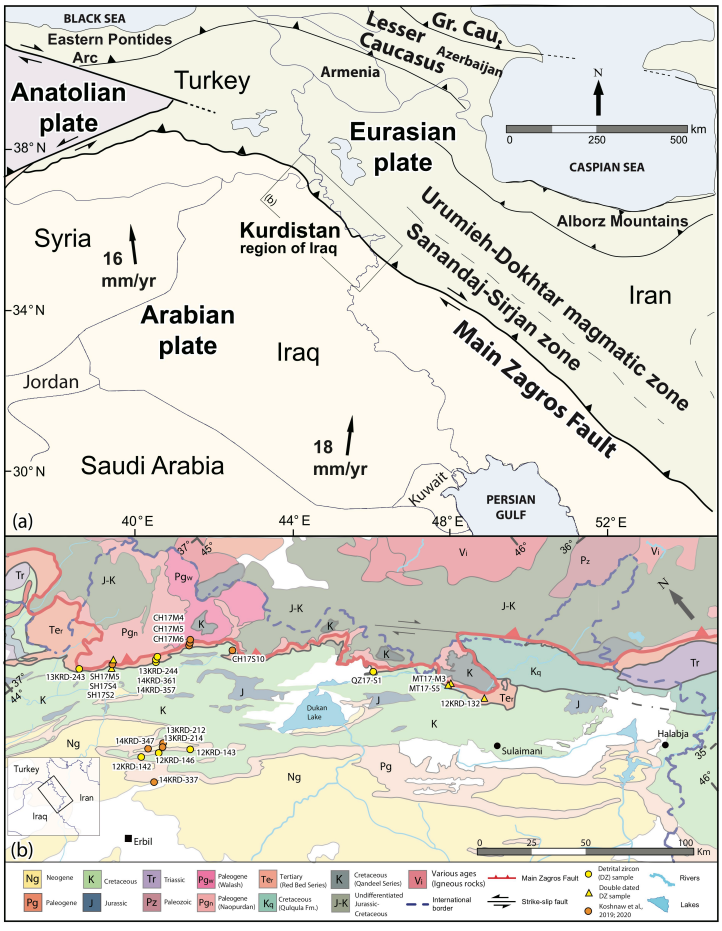

Figure 1. (a) Regional tectonic map of the Middle East displaying the study area, Kurdistan region of Iraq, and the suture of the Arabian and Eurasian plates along the Main Zagros fault (Koshnaw et al., 2017, and references therein). (b) Geologic map of the NW Zagros in the Kurdistan region of Iraq showing sample locations, new (yellow) and published (orange) (Koshnaw et al., 2019, 2020a, and references therein).

https://doi.org/10.5194/se-2021-68
Preprint. Discussion started: 19 May 2021

Solid Earth Discussions

505

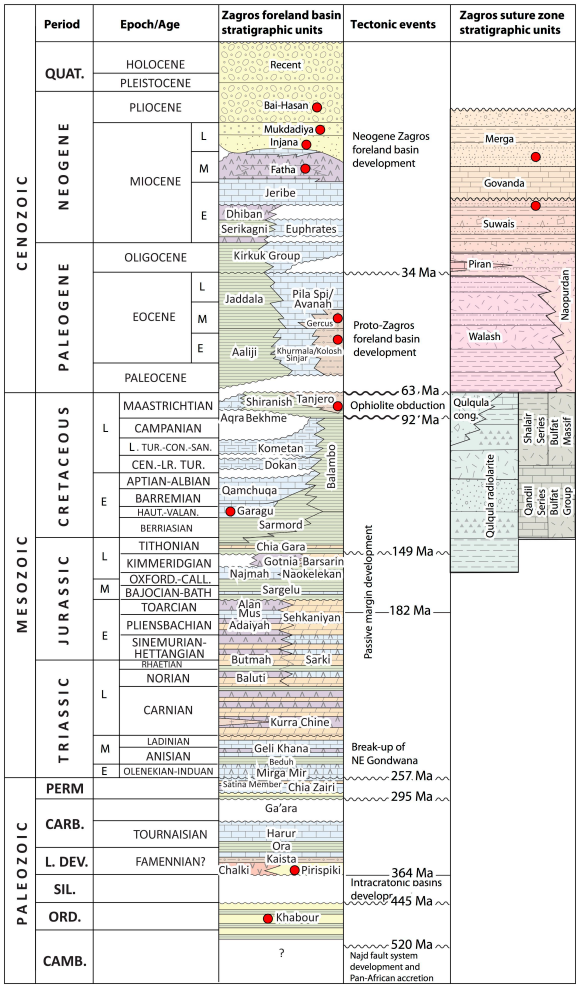

Figure 2. Generalized Phanerozoic stratigraphic column and key tectonic events for the NW Zagros fold-thrust belt and foreland basin, including the suture zone in the Kurdistan region of Iraq (Sissakian et al., 1997; Sharland et al., 2001; English et al., 2015). Red circles
510 represent stratigraphic units that were addressed in this research.

515

https://doi.org/10.5194/se-2021-68
Preprint. Discussion started: 19 May 2021

Solid Earth
Discussions
Open Access
EGU

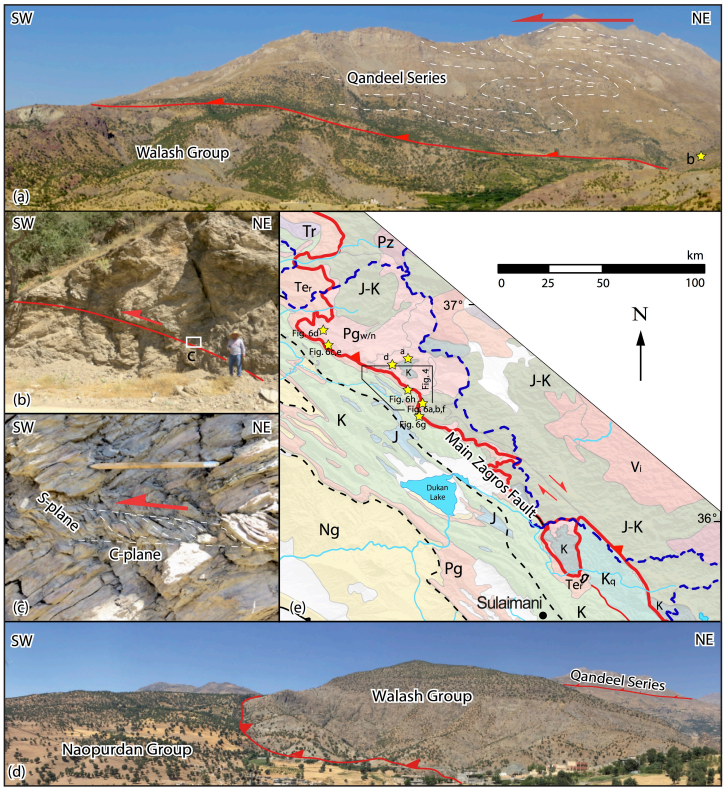

520

Figure 3. Landscape and outcrop photos exhibiting (a-d) main transported thrust sheets and their interpreted direction of motion (c, top-SW sense of shear) in the NW Zagros suture zone. (e) Simplified geologic map showing field photograph locations (yellow star).

525

530

https://doi.org/10.5194/se-2021-68
Preprint. Discussion started: 19 May 2021

Solid Earth
Discussions
Open Access
EGU

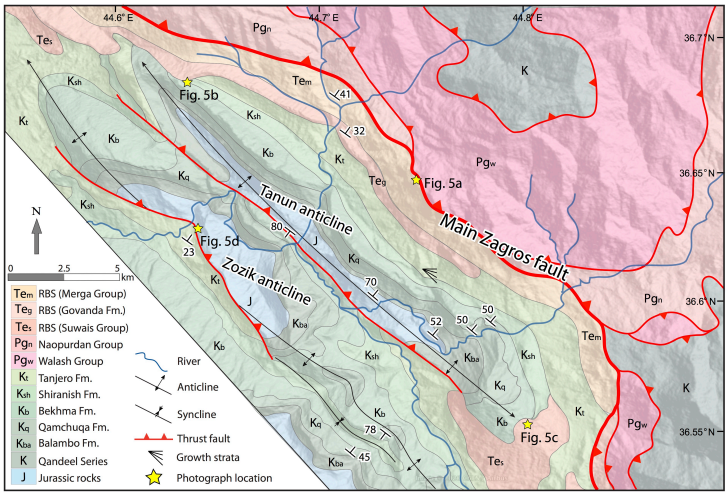

Figure 4. Geologic map illustrating key structural features, growth strata location of the Tanjero Formation (Le Garzic et al., 2019), and angular unconformity locations in the vicinity of the northwestern and southeastern plunges of the Tanun anticline.

535

540

545

550

https://doi.org/10.5194/se-2021-68
Preprint. Discussion started: 19 May 2021

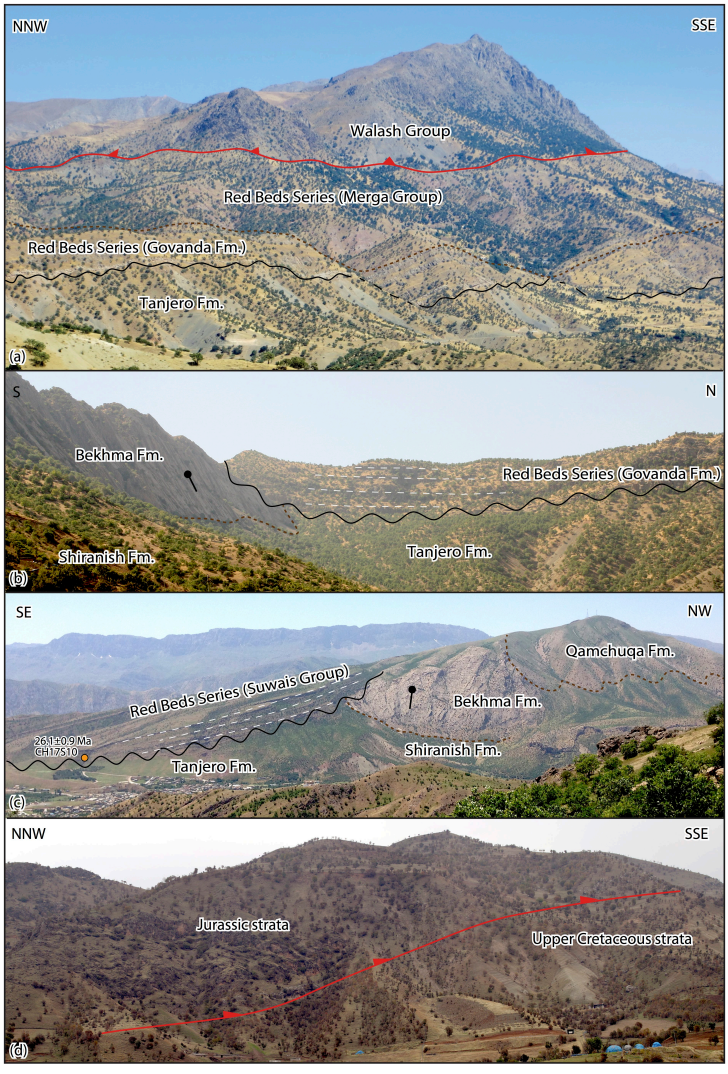

Figure 5. Landscape photographs showing field relationships. (a) The transported Paleogene Walash Group thrusted onto the Miocene units of the Red Beds Series that deposited on the Maastrichtian Tanjero Formation. (b) Angular unconformity between the middle Miocene Govanda Formation of the Red Beds Series and the folded Cretaceous units. (c) Angular unconformity between the upper Oligocene-lower Miocene (?) Suwais Group of the Red Beds Series and the folded Cretaceous units. (d) Thrust fault between the Lower Jurassic Sehkaniyan Formation and the Maastrichtian Tanjero Formation.

https://doi.org/10.5194/se-2021-68
Preprint. Discussion started: 19 May 2021

560 Figure 6. Landscape and outcrop photos displaying field examples of (a, b) Walash Group, (c, d, e) Naopurdan Group, Red Beds Series units of (f, h) Merga Group and (g) Suwais Group. The pencil cleavage tectonic fabric (e) developed in the lower part of the Naopurdan Group that thrusted onto the Merga Group. The C-S fabric developed below in the upper part of Merga Group that overlain by the thrusted Walash Group.

565

https://doi.org/10.5194/se-2021-68
Preprint. Discussion started: 19 May 2021

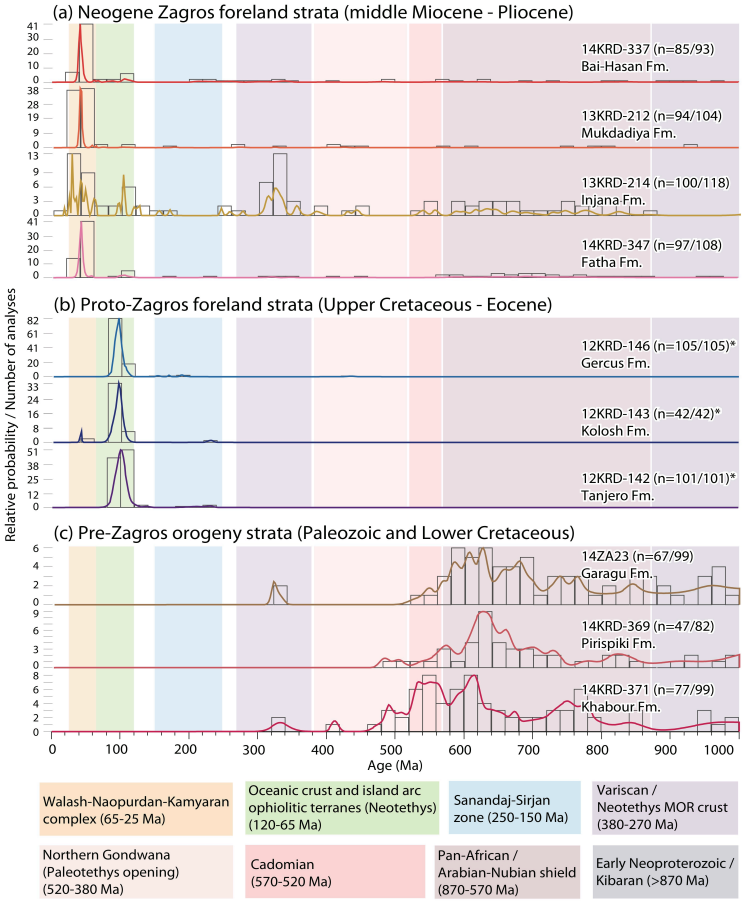

Figure 7. Detrital zircon U-Pb age distribution plots for the (a) Neogene Zagros foreland basin, (b) proto-Zagros foreland basin, and (c) pre-Zagros orogeny deposits depicted as probability density plot (PDP; bandwidth = 20, bin width = 20) and age histograms (Vermeesch, 2012). Color shading represents key source terrane age components. Samples with asterisk are new samples. Published samples are from Koshnaw et al. (2020a). Sample locations shown in Fig. 1b.

https://doi.org/10.5194/se-2021-68
Preprint. Discussion started: 19 May 2021

Solid Earth
Discussions
Open Access
EGU

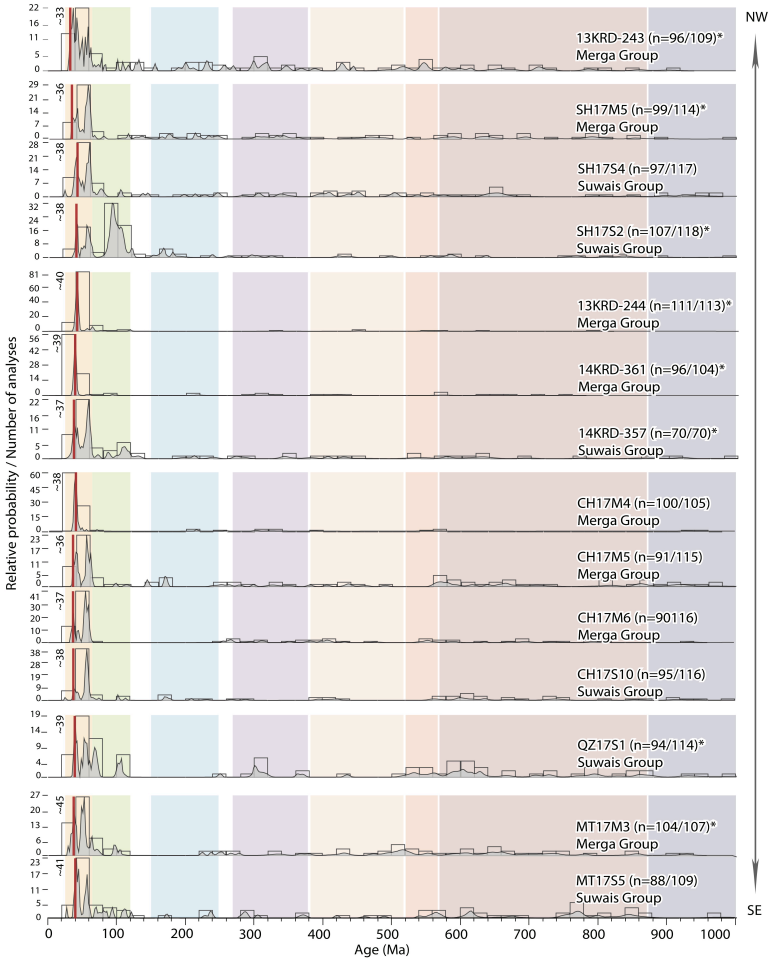

Figure 8. Detrital zircon U-Pb age distribution plots for the Red Beds Series units of the Suwais and Merga Groups depicted as probability density plot (PDP; bandwidth = 20, bin width = 20) and age histograms (Vermeesch, 2012). Dark red vertical bars delineate youngest age peak (≥3 grains). Color shading represents key source terrane age components. Samples with asterisk are new samples. Published samples are from Koshnaw et al. (2019). Sample sets are separated by white space according to their localities. Sample locations shown in Fig. 1b.

https://doi.org/10.5194/se-2021-68
Preprint. Discussion started: 19 May 2021

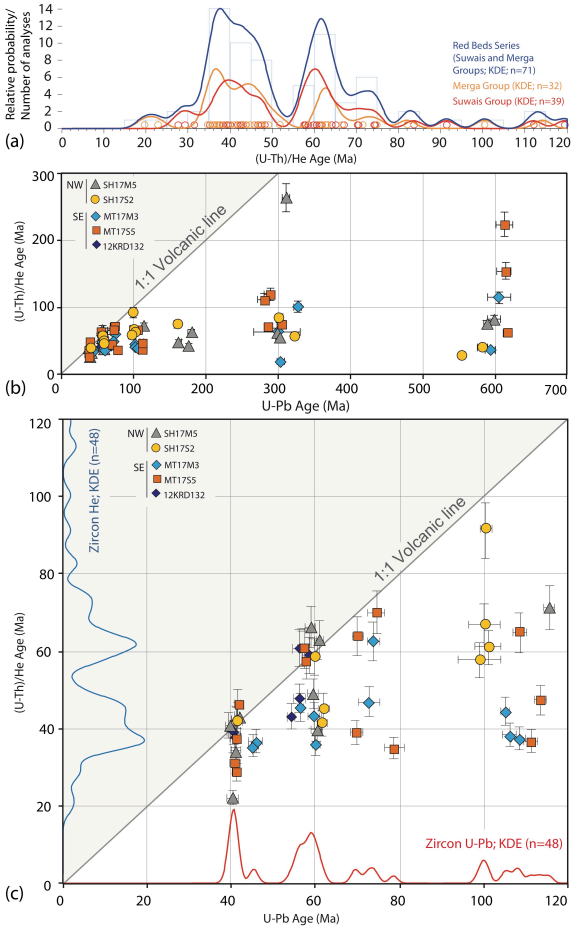

Figure 9. (a) Detrital zircon (U-Th)/He age distribution plots for the Red Beds Series units of the Suwais and Merga Groups depicted as kernel density estimation (KDE; bandwidth = 2, bin width = 5) and age histograms (Vermeesch, 2012). (b) Detrital zircon (U-Th)/(He-Pb) double dating plots of individual zircon analysis. (c) Expanded view of 0-120 Ma period to show detrital zircon (U-Th)/(He-Pb) ages for the Late Mesozoic and Cenozoic times.

https://doi.org/10.5194/se-2021-68
Preprint. Discussion started: 19 May 2021

Solid Earth
Discussions
Open Access
EGU

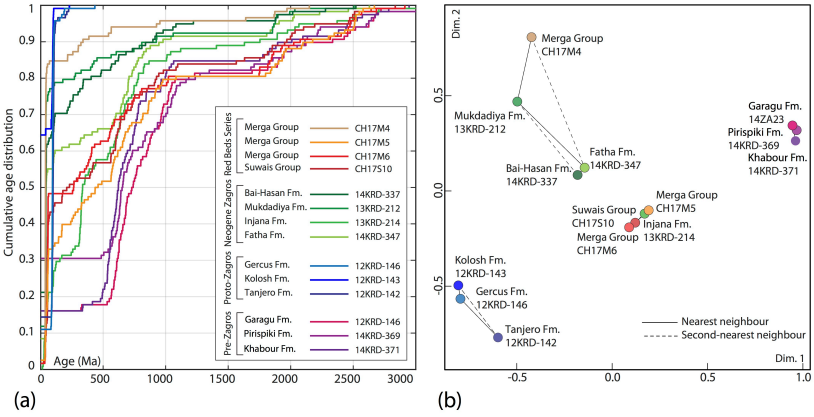

Figure 10. Comparison plots of the pre-Zagros orogeny, proto-Zagros foreland basin, Neogene Zagros foreland basin, and Red Beds Series deposits in the present-day Zagros hinterland. (a) Detrital zircon U-Pb cumulative age distribution (Saylor and Sundell, 2016). (b) Two-dimensional multidimensional scaling plot depicting relative statistical similarity/dissimilarity based on Komolgorov-Smirnov test *D* value (Vermeesch, 2013) of the detrital zircon U-Pb ages for the same sample sets in the cumulative age distribution plot. Dimension 1 and 2 are unitless.

https://doi.org/10.5194/se-2021-68
Preprint. Discussion started: 19 May 2021

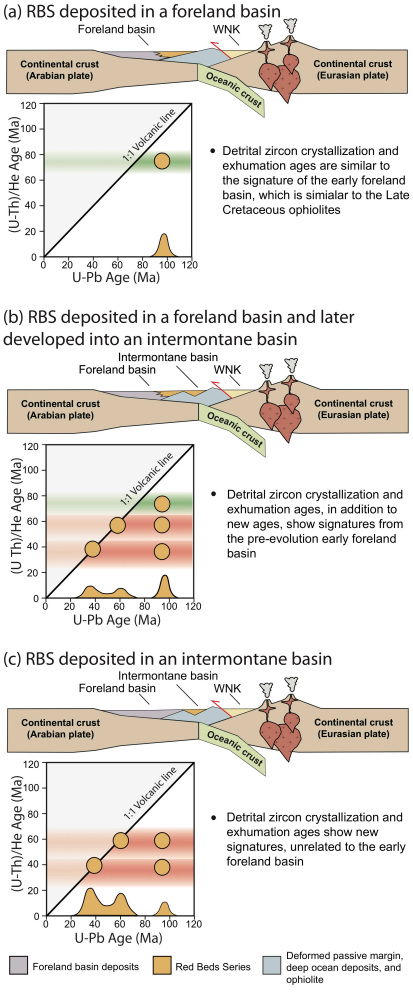

Figure 11. Predicted detrital zircon (U-Th)/(He-Pb) double dating ages for competitive hypothesis of the Red Beds Series deposited in (a) a foreland basin, (b) a foreland basin, but later partitioned and evolved into an intermontane basin, (c) an intermontane basin.

https://doi.org/10.5194/se-2021-68
Preprint. Discussion started: 19 May 2021

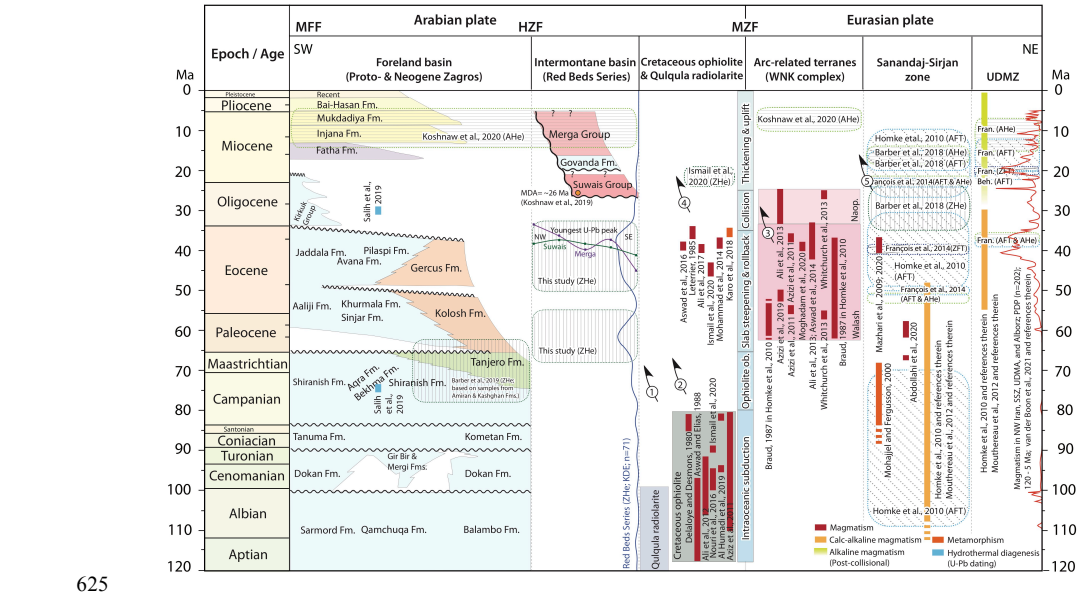

Figure 12. Time-space chart synthesizing hinterland basins stratigraphy and structural zones thermochronological and geochronological constraints on key tectonic and geodynamic, metamorphic, magmatic, and exhumational events in the broader NW Zagros sector. Numbered arrows represent estimated relative timing of the terrane thrusting. MDA, maximum depositional age; MFF, mountain front flexure; HZF, high Zagros fault; MZF, main Zagros fault; WNK, Walash-Naopurdan-Kamyaran; UDMZ, Urumieh-Dokhtar magmatic zone.

https://doi.org/10.5194/se-2021-68
Preprint. Discussion started: 19 May 2021

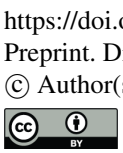

Solid Earth
Discussions
Open Access
EGU

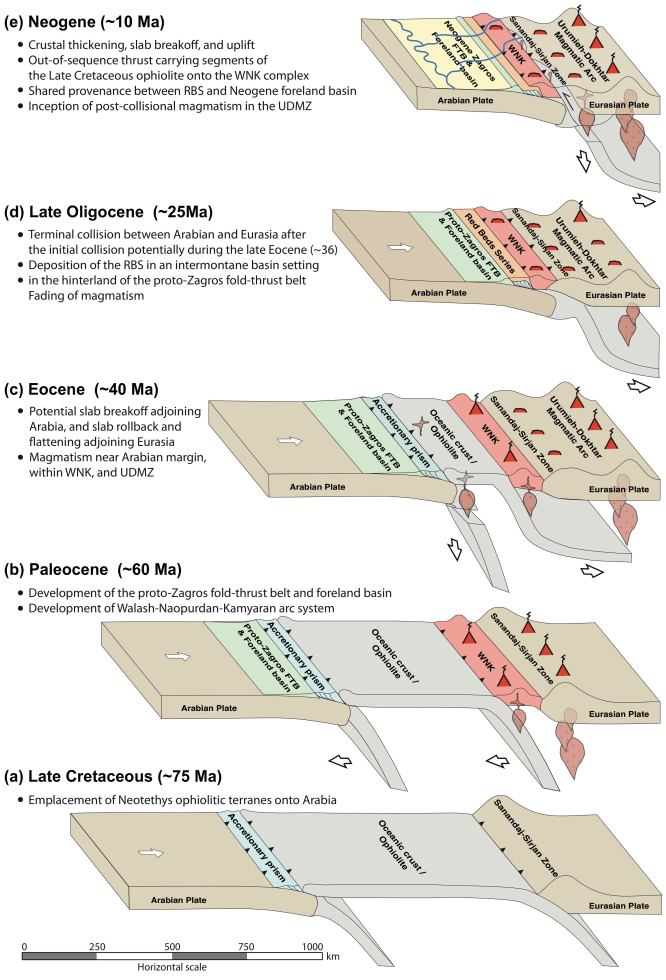

Figure 13. Schematic illustrations portraying the Late Mesozoic-Cenozoic history of the Arabia-Eurasia convergence and the present-day NW Zagros evolution. The possible configuration of the subducted Neotethys oceanic slabs, and the Arabian and Eurasian plate margins are constrained by results of this study and previous data and interpretations (Agard et al., 2005; Omrani et al., 2008; Agard et al., 2011; Moghadam and Stern, 2011; Mouthereau et al., 2012; Whitechurch et al, 2013; Ali et al., 2014; Hassanzadeh and Vernicke, 2016; and references in Fig. 12).

https://doi.org/10.5194/se-2021-68
Preprint. Discussion started: 19 May 2021

References

Abdallah, F.T. and Al-Dulaimi, S.I., 2019. Biostratigraphy of the Upper Cretaceous for selected sections in northern Iraq. Iraqi Journal of Science, pp.545-553.

Abdel-Kireem, M.R., 1986. Planktonic foraminifera and stratigraphy of the Tanjero Formation (Maastrichtian), northeastern Iraq. Micropaleontology, 32(3), pp.215-231.

Abdollahi, F., Nabatian, G., Li, J.W., Honarmand, M. and Ebrahimi, M., 2020. Saheb Granitoid Batholith, North of Kurdistan: An Evidence of Cretaceous-Paleocene Magmatism in the Sanandaj-Sirjan Zone. Journal Of Economic Geology, 12(3), pp.359-376.

Abdula, R.A., Chicho, J., Surdashy, A., Nourmohammadi, M.S., Hamad, E., Muhammad, M.M., Smail, A.A. and Ashoor, A., 2018. Sedimentology of the Govanda Formation at Gali Baza locality, Kurdistan region, Iraq. Iraqi Bulletin of Geology and Mining, 14(1), pp.1-12.

Agard, P., Omrani, J., Jolivet, L. and Mouthereau, F., 2005. Convergence history across Zagros (Iran): constraints from collisional and earlier deformation. International journal of earth sciences, 94(3), pp.401-419.

Agard, P., Omrani, J., Jolivet, L., Whitechurch, H., Vrielynck, B., Spakman, W., Monié, P., Meyer, B. and Wortel, R., 2011. Zagros orogeny: a subduction-dominated process. Geological Magazine, 148(5-6), pp.692-725.

Al Humadi, H., Väisänen, M., Ismail, S.A., Kara, J., O'Brien, H., Lahaye, Y. and Lehtonen, M., 2019. U–Pb geochronology and Hf isotope data from the Late Cretaceous Mawat ophiolite, NE Iraq. Heliyon, 5(11), p.e02721.

Al-Banna, N.Y. and M. M. Al-Mutwali, 2008. Microfacies and age determination of the sedimentary sequences within Walash volcano-sedimentary Group, Mawat Complex, northeast Iraq. Tikrit Journal of Pure Science, 13(3).

Al-Bassam, K.S., 2010. Petrology, geochemistry and depositional environment of the Khabour Formation in Ora and Khabour localities, Northern Iraq. Iraqi Bulletin of Geology and Mining, 6(2), pp.71-94.

Al-Hadide, A. H., A. I. Al-Juboury and M. I. Al-Eisa, 2002. Stratigraphic sequence of late Paleozoic era in Iraq. Iraqi National Journal of Earth Sciences, 2(1), pp.28-42.

Al-Hadidy, A.H., 2007. Paleozoic stratigraphic lexicon and hydrocarbon habitat of Iraq. GeoArabia, 12(1), pp.63-130.

Al-Juboury, A.I., Morton, A., Shingaly, W.S., Howard, J., Thusu, B., Vincent, S. and Fanning, M., 2020. Stratigraphy and age revision of the Pirispiki Formation, Kurdistan Region, Northern Iraq. Arabian Journal of Geosciences, 13(14), pp.1-15.

Al-Mashaikie, S. Z. A. K., A. T. A. Al-Azzawi, and A. K. Kadum, 2014. Depositional Environment of the Gercus Formation in Jabal Haibat Sultan, NE Iraq; New Sedimentological Approach. Iraqi Journal of Science, 55(2A), pp.471-483.

Al-Qayim, B. and A. Saadallah, 1994. Sedimentary faces and evolution of an active margin buildup, Aqra-Bekhme Formation, N. E. Iraq. Iraqi Geological Journal, 27(1), pp. 1-28.

Al-Qayim, B., Omer, A. and Koyi, H., 2012. Tectonostratigraphic overview of the Zagros suture zone, Kurdistan region, Northeast Iraq. GeoArabia, 17(4), pp.109-156.

Al-Qayim, B.A., Al-Mutwali, M.M. and Nissan, B.Y., 2008. Flysch–Molasse sediments of the Paleogene foreland basin of north Arabia, Shiranish area, north Iraq. Iraqi Bulletin of Geology and Mining, 4(1), pp.1-20.

Al-Shaibani, S., B. Al-Qayim, 1990. Micropaleontology of Tertiary-Cretaceous transect, Dokan area, northeastern Iraq. Iraqi Journal of Science, 31(2).

Ali, S.A., Buckman, S., Aswad, K.J., Jones, B.G., Ismail, S.A. and Nutman, A.P., 2012. Recognition of Late Cretaceous Hasanbag ophiolite-arc rocks in the Kurdistan Region of the Iraqi Zagros suture zone: A missing link in the paleogeography of the closing Neotethys Ocean. Lithosphere, 4(5), pp.395-410.

Ali, S.A., Buckman, S., Aswad, K.J., Jones, B.G., Ismail, S.A. and Nutman, A.P., 2013. The tectonic evolution of a N eo-T ethyan (E ocene–O ligocene) island-arc (W alash and N aopurdan groups) in the K urdistan region of the N ortheast I raqi Z agros S uture Z one. Island Arc, 22(1), pp.104-125.

https://doi.org/10.5194/se-2021-68
Preprint. Discussion started: 19 May 2021

Ali, S.A., Mohajjel, M., Aswad, K., Ismail, S., Buckman, S. and Jones, B., 2014. Tectono-stratigraphy and structure of the northwestern Zagros collision zone across the Iraq-Iran border.

Ali, S.A., Nutman, A.P., Aswad, K.J. and Jones, B.G., 2019. Overview of the tectonic evolution of the Iraqi Zagros thrust zone: Sixty million years of Neotethyan ocean subduction. Journal of Geodynamics, 129, pp.162-177.

Ali, S.A., Sleabi, R.S., Talabani, M.J. and Jones, B.G., 2017. Provenance of the Walash-Naopurdan back-arc–arc clastic sequences in the Iraqi Zagros Suture Zone. Journal of African Earth Sciences, 125, pp.73-87.

Allen, M.B. and Armstrong, H.A., 2008. Arabia–Eurasia collision and the forcing of mid-Cenozoic global cooling. Palaeogeography, Palaeoclimatology, Palaeoecology, 265(1-2), pp.52-58.

Alsultan, H.A.A. and Ali, D., 2016. Basin Development of the Red Bed Series, Ne Iraq. Journal of University of Babylon, 24(2).

Ameen, B.M., 2009. Lthological indicators for the Oligocene unconformity, NE Iraq. Iraqi Bulletin of Geology and Mining, 5(1), pp.25-34.

Ameen, M.S., 1992. Effect of basement tectonics on hydrocarbon generation, migration, and accumulation in northern Iraq. AAPG bulletin, 76(3), pp.356-370.

Aqrawi, A.A., Goff, J.C., Horbury, A.D. and Sadooni, F.N., 2010. The petroleum geology of Iraq. Scientific Press.

Aswad, K.J. and Elias, E.M., 1988. Petrogenesis, geochemistry and metamorphism of spilitized subvolcanic rocks of the Mawat Ophiolite Complex, NE Iraq. Ofioliti, 13(2/3), pp.95-109.

Aswad, K.J., Al-Samman, A.H., Aziz, N.R. and Koyi, A.M., 2014. The geochronology and petrogenesis of Walash volcanic rocks, Mawat nappes: constraints on the evolution of the northwestern Zagros suture zone, Kurdistan Region, Iraq. Arabian Journal of Geosciences, 7(4), pp.1403-1432.

Avigad, D., Abbo, A. and Gerdes, A., 2016. Origin of the Eastern Mediterranean: Neotethys rifting along a cryptic Cadomian suture with Afro-Arabia. Bulletin, 128(7-8), pp.1286-1296.

Avigad, D., Morag, N., Abbo, A. and Gerdes, A., 2017. Detrital rutile U-Pb perspective on the origin of the great Cambro-Ordovician sandstone of North Gondwana and its linkage to orogeny. Gondwana Research, 51, pp.17-29.

Avouac, J.P. and Burov, E.B., 1996. Erosion as a driving mechanism of intracontinental mountain growth. Journal of Geophysical Research: Solid Earth, 101(B8), pp.17747-17769.

Avouac, J.P., Meng, L., Wei, S., Wang, T. and Ampuero, J.P., 2015. Lower edge of locked Main Himalayan Thrust unzipped by the 2015 Gorkha earthquake. Nature Geoscience, 8(9), pp.708-711.

Aziz, N.H., 2020. U-Pb Zircon Dating of Upper Cretaceous Siliciclastic Rocks from the Tanjero Flysch, NE Iraq: New Constraints on their Provenance, and Tectonic Evolution. Kuwait Journal of Science, 47(4).

Aziz, N.R., Elias, E.M. and Aswad, K.J., 2011. Rb-Sr and Sm-Nd isotopes study of serpentinites and their impact on the tectonic setting of Zagros suture zone, NE Iraq. Iraqi Bulletin of Geology and Mining, 7(1), pp.67-75.

Azizi, H., Hadad, S., Stern, R.J. and Asahara, Y., 2019. Age, geochemistry, and emplacement of the~ 40-Ma Baneh granite–appinite complex in a transpressional tectonic regime, Zagros suture zone, northwest Iran. International Geology Review, 61(2), pp.195-223.

Azizi, H., Hadi, A., Asahara, Y. and Mohammad, Y., 2013. Geochemistry and geodynamics of the Mawat mafic complex in the Zagros Suture zone, northeast Iraq. Open Geosciences, 5(4), pp.523-537.

Azizi, H., Tanaka, T., Asahara, Y., Chung, S.L. and Zarrinkoub, M.H., 2011. Discrimination of the age and tectonic setting for magmatic rocks along the Zagros thrust zone, northwest Iran, using the zircon U–Pb age and Sr–Nd isotopes. Journal of Geodynamics, 52(3-4), pp.304-320.

Ballato, P., Uba, C.E., Landgraf, A., Strecker, M.R., Sudo, M., Stockli, D.F., Friedrich, A. and Tabatabaei, S.H., 2011. Arabia-Eurasia continental collision: Insights from late Tertiary foreland-basin evolution in the Alborz Mountains, northern Iran. Bulletin, 123(1-2), pp.106-131.

https://doi.org/10.5194/se-2021-68
Preprint. Discussion started: 19 May 2021

Barber, D.E., Stockli, D.F. and Galster, F., 2019. The Proto-Zagros foreland basin in Lorestan, western Iran: Insights from multimineral detrital geothermochronometric and trace elemental provenance analysis. Geochemistry, Geophysics, Geosystems, 20(6), pp.2657-2680.

Barber, D.E., Stockli, D.F., Horton, B.K. and Koshnaw, R.I., 2018. Cenozoic exhumation and foreland basin evolution of the Zagros orogen during the Arabia-Eurasia collision, western Iran. Tectonics, 37(12), pp.4396-4420.

Behyari, M., Mohajjel, M., Sobel, E.R., Rezaeian, M., Moayyed, M. and Schmidt, A., 2017. Analysis of exhumation history in Misho Mountains, NW Iran: Insights from structural and apatite fission track data. Neues Jb Geol Paläontol Abh, 283, pp.291-308.

Braud, J. 1987. La Suture Du Zagros Au Niveau De Kermanshah (Kurdistan Iranien): Reconstitution Paleogeographique, Evolution Geodynamique, Magmatique Et Structurale. Unpublished PhDThesis, Universtie Paris-Sud, 488pp.

Braud, J.E.A.N. and Ricou, L.E., 1975. Eléments de continuité entre le Zagros et la Turquie du Sud-Est. Bulletin de la Societe Geologique de France, 7(6), pp.1015-1023.

Cawood, P.A., Hawkesworth, C.J. and Dhuime, B., 2012. Detrital zircon record and tectonic setting. Geology, 40(10), pp.875-878.

Çelik, H. and SALİH, T.M.H., 2018. Provenance investigation from sedimentary petrography of the Upper Cretaceous deep marine low density turbidites of the Tanjero Formation around Arbat, northeastern Iraq. Turkish Journal of Earth Sciences, 27(6), pp.432-459.

Çelik, H. and SALİH, T.M.H., 2021. Petrographic characteristics of deep marine turbidite sandstones of the Upper Cretaceous Tanjero Formation, Northwestern Sulaimaniyah, Iraq: implications for provenance and tectonic setting. Bulletin of the Mineral Research and Exploration, 164-?

Chiu, H.Y., Chung, S.L., Zarrinkoub, M.H., Mohammadi, S.S., Khatib, M.M. and Iizuka, Y., 2013. Zircon U–Pb age constraints from Iran on the magmatic evolution related to Neotethyan subduction and Zagros orogeny. Lithos, 162, pp.70-87.

Cloos, M., 1993. Lithospheric buoyancy and collisional orogenesis: Subduction of oceanic plateaus, continental margins, island arcs, spreading ridges, and seamounts. Geological Society of America Bulletin, 105(6), pp.715-737.

Colleps, C.L., McKenzie, N.R., Horton, B.K., Webb, A.A.G., Ng, Y.W. and Singh, B.P., 2020. Sediment provenance of pre- and post-collisional Cretaceous–Paleogene strata from the frontal Himalaya of northwest India. Earth and Planetary Science Letters, 534, p.116079.

Darin, M.H., Umhoefer, P.J. and Thomson, S.N., 2018. Rapid late Eocene exhumation of the Sivas Basin (Central Anatolia) driven by initial Arabia-Eurasia collision. Tectonics, 37(10), pp.3805-3833.

DeCelles, P.G., Carrapa, B., Horton, B.K., McNabb, J., Gehrels, G.E. and Boyd, J., 2015. The Miocene Arizaro Basin, central Andean hinterland: Response to partial lithosphere removal. Geol. Soc. Am. Mem, 212, pp.359-386.

Delaloye, M. and Desmons, J., 1980. Ophiolites and mélange terranes in Iran: a geochronological study and its paleotectonic implications. Tectonophysics, 68(1-2), pp.83-111.

Dercourt, J., Zonenshain, L.P., Ricou, L.E., Kazmin, V.G., Le Pichon, X., Knipper, A.L., Grandjacquet, C., Sbortshikov, I.M., Geyssant, J., Lepvrier, C. and Pechersky, D.H., 1986. Geological evolution of the Tethys belt from the Atlantic to the Pamirs since the Lias. Tectonophysics, 123(1-4), pp.241-315.

Dewey, J.F., PITMAN III, W.C., Ryan, W.B. and Bonnin, J., 1973. Plate tectonics and the evolution of the Alpine system. Geological society of America bulletin, 84(10), pp.3137-3180.

Dunnington, H. V., 1958. Generation, migration, accumulation and dissipation of oil in northern Iraq, in Weeks, L. G., editor, Habitat of oil, a symposium: Tulsa, American Association of Petroleum Geologists, p. 1149–1251.

English, J.M., Lunn, G.A., Ferreira, L. and Yacu, G., 2015. Geologic evolution of the Iraqi Zagros, and its influence on the distribution of hydrocarbons in the Kurdistan region. AAPG Bulletin, 99(2), pp.231-272.

https://doi.org/10.5194/se-2021-68
Preprint. Discussion started: 19 May 2021

Farley, K.A., Wolf, R.A. and Silver, L.T., 1996. The effects of long alpha-stopping distances on (U-Th)/He ages. Geochimica et cosmochimica acta, 60(21), pp.4223-4229.

Francois, T., Agard, P., Bernet, M., Meyer, B., Chung, S.L., Zarrinkoub, M.H., Burov, E. and Monie, P., 2014. Cenozoic exhumation of the internal Zagros: first constraints from low-temperature thermochronology and implications for the build-up of the Iranian plateau. Lithos, 206, pp.100-112.

Gehrels, G., 2014. Detrital zircon U-Pb geochronology applied to tectonics. Annual Review of Earth and Planetary Sciences, 42, pp.127-149.

Gehrels, G.E., 2000. Introduction to detrital zircon studies of Paleozoic and Triassic strata in western Nevada and northern California. Special Paper of the Geological Society of America, 347, pp.1-17.

Grimes, C.B., John, B.E., Kelemen, P.B., Mazdab, F.K., Wooden, J.L., Cheadle, M.J., Hanghøj, K. and Schwartz, J.J., 2007. Trace element chemistry of zircons from oceanic crust: A method for distinguishing detrital zircon provenance. Geology, 35(7), pp.643-646.

Hart, N.R., Stockli, D.F. and Hayman, N.W., 2016. Provenance evolution during progressive rifting and hyperextension using bedrock and detrital zircon U-Pb geochronology, Mauléon Basin, western Pyrenees. Geosphere, 12(4), pp.1166-1186.

Hassan, M.M., Jones, B.G., Buckman, S., Al-Jubory, A.I. and Al Gahtani, F.M., 2014. Provenance of Paleocene–Eocene red beds from NE Iraq: constraints from framework petrography. Geological Magazine, 151(6), pp.1034-1050.

Hassanzadeh, J. and Wernicke, B.P., 2016. The Neotethyan Sanandaj-Sirjan zone of Iran as an archetype for passive margin-arc transitions. Tectonics, 35(3), pp.586-621.

Hempton, M.R., 1985. Structure and deformation history of the Bitlis suture near Lake Hazar, southeastern Turkey. Geological Society of America Bulletin, 96(2), pp.233-243.

Hempton, M.R., 1987. Constraints on Arabian plate motion and extensional history of the Red Sea. Tectonics, 6(6), pp.687-705.

Homke, S., Vergés, J., Van Der Beek, P., Fernàndez, M., Saura, E., Barbero, L., Badics, B. and Labrin, E., 2010. Insights in the exhumation history of the NW Zagros from bedrock and detrital apatite fission-track analysis: evidence for a long-lived orogeny. Basin Research, 22(5), pp.659-680.

Horton, B.K., Busby, C. and Azor, A., 2012. Cenozoic evolution of hinterland basins in the Andes and Tibet. Tectonics of sedimentary basins: recent advances, pp.427-444.

Horton, B.K., Hassanzadeh, J., Stockli, D.F., Axen, G.J., Gillis, R.J., Guest, B., Amini, A., Fakhari, M.D., Zamanzadeh, S.M. and Grove, M., 2008. Detrital zircon provenance of Neoproterozoic to Cenozoic deposits in Iran: Implications for chronostratigraphy and collisional tectonics. Tectonophysics, 451(1-4), pp.97-122.

Ismail, Sabah A., Renas I. Koshnaw, Douglas E. Barber, Heider Al Humadi, and Daniel F. Stockli. "Generation and exhumation of granitoid intrusions in the Penjween ophiolite complex, NW Zagros of the Kurdistan region of Iraq: Implications for the geodynamic evolution of the Arabian-Eurasian collision zone." Lithos 376 (2020): 105714.

Jassim, S. Z. and V. Sisakian, 1978. Field guide to the geology of Salah Al-Din-Shaqlawa area, northeastern Iraq. Geological society of Iraq and Union of Iraqi Geologists, Fifth Iraqi geological congress, Baghdad, Iraq

Jassim, S. Z., and Buday, T., 2006. Units of the unstable shelf and the Zagros suture. In: Jassim, S.Z., Goff, J.C. (Eds.), Geology of Iraq. Dolin and Moravian Museum, Prague and Brno, Czech Republic, pp. 73–90.

Jassim, S.Z., Buday, T., Cicha, I., Opletal, M., 2006. Tectonostratigraphy of the Zagros suture. In: Jassim, S.Z., Goff, J.C. (Eds.), Geology of Iraq. Dolin and Moravian Museum, Prague and Brno, Czech Republic, pp. 276–29

Jones, B.G., Ali, S.A. and Nutman, A.P., 2020. Provenance of Tanjero and Red Bed clastic sedimentary rocks revealed by detrital zircon SHRIMP dating, Kurdistan region, NE Iraq: Constraints on ocean closure and unroofing of Neo-Tethyan allochthons. Journal of African Earth Sciences, 172, p.103981.

https://doi.org/10.5194/se-2021-68
Preprint. Discussion started: 19 May 2021

Kadem, L.S., 2006. Mixed carbonate clastic sediment facies of the Paleocene–L. Eocene Kolosh Formation from selected locations in North Iraq. Tikrit Journal of Pure Science, 11(2).

Karim, K.H., Al-Barzinjy, S.T. and Ameen, B.M., 2008. History and geological setting of intermontane basins in the Zagros fold–thrust belt, Kurdistan region, NE Iraq. Iraqi Bulletin of Geology and Mining, 4(1), pp.21-33.

Karim, K.H., Koyi, H., Baziany, M.M. and Hessami, K., 2011. Significance of angular unconformities between Cretaceous and Tertiary strata in the northwestern segment of the Zagros fold–thrust belt, Kurdistan Region, NE Iraq. Geological Magazine, 148(5-6), pp.925-939.

Karo, N.M., Oberhänsli, R., Aqrawi, A.M., Elias, E.M., Aswad, K.J. and Sudo, M., 2018. New 40 Ar/39 Ar age constraints on cooling and unroofing history of the metamorphic host rocks (and igneous intrusion associates) from the Bulfat Complex (Bulfat area), NE-Iraq. Arabian Journal of Geosciences, 11(10), pp.1-11.

Kharajiany SO, Al-Qayim BA, Wise Jr SW. Calcareous nannofossil stratigraphy of the Upper Cretaceous–lower Paleocene sequence from the Chinarok section, Sulaimaniah area, Kurdistan region, NE Iraq. Iraqi Bulletin of Geology and Mining. 2019 Sep 25;15(1):1-4.

Konert, G., Afifi, A.M., Al-Hajri, S.I.A. and Droste, H.J., 2001. Paleozoic stratigraphy and hydrocarbon habitat of the Arabian Plate. GeoArabia, 6(3), pp.407-442.

Koshnaw, R.I., Horton, B.K., Stockli, D.F., Barber, D.E. and Tamar-Agha, M.Y., 2020a. Sediment routing in the Zagros foreland basin: Drainage reorganization and a shift from axial to transverse sediment dispersal in the Kurdistan region of Iraq. Basin Research, 32(4), pp.688-715.

Koshnaw, R.I., Horton, B.K., Stockli, D.F., Barber, D.E., Tamar-Agha, M.Y. and Kendall, J.J., 2017. Neogene shortening and exhumation of the Zagros fold-thrust belt and foreland basin in the Kurdistan region of northern Iraq. Tectonophysics, 694, pp.332-355.

Koshnaw, R.I., Stockli, D.F. and Schlunegger, F., 2019. Timing of the Arabia-Eurasia continental collision—Evidence from detrital zircon U-Pb geochronology of the Red Bed Series strata of the northwest Zagros hinterland, Kurdistan region of Iraq. Geology, 47(1), pp.47-50.

Koshnaw, R.I., Stockli, D.F., Horton, B.K., Teixell, A., Barber, D.E. and Kendall, J.J., 2020b. Late Miocene Deformation Kinematics Along the NW Zagros Fold-Thrust Belt, Kurdistan Region of Iraq: Constraints From Apatite (U-Th)/He Thermochronometry and Balanced Cross Sections. Tectonics, 39(12), p.e2019TC005865.

Koyi, A.M., 2009. Sr-Nd isotopical significance of Walash volcanic rocks, Mawat area, NE Iraq. Zanco J. Pure Appl. Sci. 21, 39–45.

Lawa, F.A., Koyi, H. and Ibrahim, A., 2013. Tectono-stratigraphic evolution of the NW segment OF the Zagros fold-thrust belt, Kurdistan, NE Iraq. Journal of Petroleum Geology, 36(1), pp.75-96.

Le Garzic, E., Vergés, J., Sapin, F., Saura, E., Meresse, F. and Ringenbach, J.C., 2019. Evolution of the NW Zagros Fold-and-Thrust Belt in Kurdistan Region of Iraq from balanced and restored crustal-scale sections and forward modeling. Journal of Structural Geology, 124, pp.51-69.

Leterrier, J., 1985. Mineralogical, geochemical and isotopic evolution of two Miocene mafic intrusions from the Zagros (Iran). Lithos, 18, pp.311-329.

Liu, S., Su, S. and Zhang, G., 2013. Early Mesozoic basin development in North China: Indications of cratonic deformation. Journal of Asian Earth Sciences, 62, pp.221-236.

Karim, H. K. and A. M. Surdashy, 2005. Paleocurrent Analysis of Upper Cretaceous Zagros Foreland Basin: A Case Study for Tanjero Formation in Sulaimaniya Area NE-Iraq. Iraqi National Journal of Earth Sciences, 5(1), pp.30-44.

Marsh, J.H. and Stockli, D.F., 2015. Zircon U–Pb and trace element zoning characteristics in an anatectic granulite domain: Insights from LASS-ICP-MS depth profiling. Lithos, 239, pp.170-185.

https://doi.org/10.5194/se-2021-68
Preprint. Discussion started: 19 May 2021

Mazhari, S.A., Bea, F., Amini, S., Ghalamghash, J., Molina, J.F., Montero, P., Scarrow, J.H. and Williams, I.S., 2009. The Eocene bimodal Piranshahr massif of the Sanandaj–Sirjan Zone, NW Iran: a marker of the end of the collision in the Zagros orogen. Journal of the Geological Society, 166(1), pp.53-69.

Mazhari, S.A., Ghalamghash, J., Kumar, S., Shellnutt, J.G. and Bea, F., 2020. Tectonomagmatic development of the Eocene Pasevh pluton (NW Iran): Implications for the Arabia-Eurasia collision. Journal of Asian Earth Sciences, 203, p.104551.

McQuarrie, N. and van Hinsbergen, D.J., 2013. Retrodeforming the Arabia-Eurasia collision zone: Age of collision versus magnitude of continental subduction. Geology, 41(3), pp.315-318.

Meinhold, G., Bassis, A., Hinderer, M., Lewin, A. and Berndt, J., 2020. Detrital zircon provenance of north Gondwana Palaeozoic sandstones from Saudi Arabia. Geological Magazine, pp.1-17.

Moghadam, H.S., Li, Q.L., Stern, R.J., Chiaradia, M., Karsli, O. and Rahimzadeh, B., 2020. The Paleogene ophiolite conundrum of the Iran–Iraq border region. Journal of the Geological Society, 177(5), pp.955-964.

Mohammad, Y.O., Cornell, D.H., Qaradaghi, J.H. and Mohammad, F.O., 2014. Geochemistry and Ar–Ar muscovite ages of the Daraban Leucogranite, Mawat Ophiolite, northeastern Iraq: implications for Arabia–Eurasia continental collision. Journal of Asian Earth Sciences, 86, pp.151-165.

Molnar, P. and England, P., 1990. Late Cenozoic uplift of mountain ranges and global climate change: chicken or egg?. Nature, 346(6279), pp.29-34.

Mouthereau, F., Lacombe, O. and Vergés, J., 2012. Building the Zagros collisional orogen: timing, strain distribution and the dynamics of Arabia/Eurasia plate convergence. Tectonophysics, 532, pp.27-60.

Müller, R.D., Cannon, J., Qin, X., Watson, R.J., Gurnis, M., Williams, S., Pfaffelmoser, T., Seton, M., Russell, S.H. and Zahirovic, S., 2018. GPlates: building a virtual Earth through deep time. Geochemistry, Geophysics, Geosystems, 19(7), pp.2243-2261.

Najman, Y., Appel, E., Boudagher-Fadel, M., Bown, P., Carter, A., Garzanti, E., Godin, L., Han, J., Liebke, U., Oliver, G. and Parrish, R., 2010. Timing of India-Asia collision: Geological, biostratigraphic, and palaeomagnetic constraints. Journal of Geophysical Research: Solid Earth, 115(B12).

Norton, K. and Schlunegger, F., 2011. Migrating deformation in the Central Andes from enhanced orographic rainfall. Nature Communications, 2(1), pp.1-7.

Nouri, F., Azizi, H., Golonka, J., Asahara, Y., Orihashi, Y., Yamamoto, K., Tsuboi, M. and Anma, R., 2016. Age and petrogenesis of Na-rich felsic rocks in western Iran: evidence for closure of the southern branch of the Neo-Tethys in the Late Cretaceous. Tectonophysics, 671, pp.151-172.

Numan, N.M., 1997. A plate tectonic scenario for the Phanerozoic succession in Iraq. Iraqi Geological Journal, 30(2), pp.85-110.

Numan, N.M.S., Hammoudi, R.A. and Chorowicz, J., 1998. Synsedimentary tectonics in the Eocene Pila Spi limestone formation in Iraq and its geodynamic implications. Journal of African Earth Sciences, 27(1), pp.141-148.

Orme, D.A., Carrapa, B. and Kapp, P., 2015. Sedimentology, provenance and geochronology of the Upper Cretaceous–Lower Eocene western Xigaze forearc basin, southern Tibet. Basin Research, 27(4), pp.387-411.

Pujols, E.J., Stockli, D.F., Constenius, K.N. and Horton, B.K., 2020. Thermochronological and geochronological constraints on Late Cretaceous unroofing and proximal sedimentation in the Sevier orogenic belt, Utah. Tectonics, 39(7), p.e2019TC005794.

Reiners, P.W., Farley, K.A. and Hickes, H.J., 2002. He diffusion and (U–Th)/He thermochronometry of zircon: initial results from Fish Canyon Tuff and Gold Butte. Tectonophysics, 349(1-4), pp.297-308.

Rolland, Y., Perincek, D., Kaymakci, N., Sosson, M., Barrier, E. and Avagyan, A., 2012. Evidence for~ 80–75 Ma subduction jump during Anatolide–Tauride–Armenian block accretion and~ 48 Ma Arabia–Eurasia collision in Lesser Caucasus–East Anatolia. Journal of Geodynamics, 56, pp.76-85.

https://doi.org/10.5194/se-2021-68
Preprint. Discussion started: 19 May 2021

Salih, N., Mansurbeg, H., Kolo, K., Gerdes, A. and Préat, A., 2020. In situ U-Pb dating of hydrothermal diagenesis in tectonically controlled fracturing in the Upper Cretaceous Bekhme Formation, Kurdistan Region-Iraq. International Geology Review, 62(18), pp.2261-2279.

Sasvari, A., Davies, L., Mann, A., Afzal, J., Vakarcs, G. and Iwaniw, E., 2015. Dachstein-type Avroman Formation: An indicator of the Harsin Basin in Iraq. GeoArabia, 20(4), pp.17-36.

Saura, E., Vergés, J., Homke, S., Blanc, E., Serra-Kiel, J., Bernaola, G., Casciello, E., Fernández, N., Romaire, I., Casini, G. and Embry, J.C., 2011. Basin architecture and growth folding of the NW Zagros early foreland basin during the Late Cretaceous and early Tertiary. Journal of the Geological Society, 168(1), pp.235-250.

Saura, E., Garcia-Castellanos, D., Casciello, E., Parravano, V., Urruela, A., & Vergés, J., 2015. Modeling the flexural evolution of the Amiran and Mesopotamian foreland basins of NW Zagros (Iran-Iraq). Tectonics, 34(3), 377-395.

Sharland, P. R., Archer, R., Casey, D. M., Davies, R. B., Hall, S. H., Heward, A. P., et al., 2001. Arabian plate sequence stratigraphy, GeoArabia, Special Publication (p. 2). Bahrain: PetroLink.

Shawkat, M. G., & Tucker, M. E., 1978. Stromatolites and sabkha cycles from the lower Fars formation (Miocene) of Iraq. Geological Review, 67(1), 1–14

Stampfli, G.M. and Borel, G.D., 2002. A plate tectonic model for the Paleozoic and Mesozoic constrained by dynamic plate boundaries and restored synthetic oceanic isochrons. Earth and Planetary Science Letters, 196(1-2), pp.17-33.

Stern, R.J., 2002. Subduction zones. Reviews of geophysics, 40(4), pp.3-1.

Stern, R.J., 2010. The anatomy and ontogeny of modern intra-oceanic arc systems. Geological Society, London, Special Publications, 338(1), pp.7-34.

Stockli, D., Boyd, P., & Galster, F. (2017). Intragrain common Pb correction in apatite by LA-ICP-MS depth profiling and implications for detrital apatite U-Pb dating. Geophysical Research Abstracts, EGU General Assembly, 19, 12225.

Tamar-Agha, M., N. M. S. Numan, and K. Malala, 1978. Field guide for the geology of Dohok and Sinjar areas. Geological society of Iraq and Union of Iraqi Geologists, Fifth Iraqi geological congress, Baghdad, Iraq

Tamar-Agha, M.Y. and Al-Aslami, O.J.M., 2015. Facies, Depositional Environment and Cyclicity of the Fatha Formation in East Baghdad Oil Field, Iraq. Iraqi Journal of Science, 56(4A), pp.2939-2952.

Tamar-Agha, M.Y. and Salman, N.A., 2015. Facies and Depositional Environments of Injana Formation in Zawita, Amadia and Zakho Areas, Northern Iraq. Iraqi Bulletin of Geology and Mining, 11(3), pp.39-60.

Thomson, K.D., Stockli, D.F., Clark, J.D., Puigdefàbregas, C. and Fildani, A., 2017. Detrital zircon (U-Th)/(He-Pb) double-dating constraints on provenance and foreland basin evolution of the Ainsa Basin, south-central Pyrenees, Spain. Tectonics, 36(7), pp.1352-1375.

van Bellen, V. R. C., Dunnington, H. V., Wetzel, R., & Morton, D. M. (1959). Lexique Stratigraphique International. 3. Asie, fasc. 10a, Iraq. CNRS (Cent. Natl. Rech. Sci.), Paris.

van der Boon, A., Kuiper, K.F., van der Ploeg, R., Cramwinckel, M.J., Honarmand, M., Sluijs, A. and Krijgsman, W., 2021. Exploring a link between the Middle Eocene Climatic Optimum and Neotethys continental arc flare-up. Climate of the Past, 17(1), pp.229-239.

Van der Meer, D.G., Van Hinsbergen, D.J. and Spakman, W., 2018. Atlas of the underworld: Slab remnants in the mantle, their sinking history, and a new outlook on lower mantle viscosity. Tectonophysics, 723, pp.309-448.

Verdel, C., Wernicke, B.P., Hassanzadeh, J. and Guest, B., 2011. A Paleogene extensional arc flare-up in Iran. Tectonics, 30(3).

Vergés, J., Saura, E., Casciello, E., Fernandez, M., Villaseñor, A., Jimenez-Munt, I. and García-Castellanos, D., 2011. Crustal-scale cross-sections across the NW Zagros belt: implications for the Arabian margin reconstruction. Geological Magazine, 148(5-6), pp.739-761.

https://doi.org/10.5194/se-2021-68
Preprint. Discussion started: 19 May 2021

Webb, A.A.G., Yin, A. and Dubey, C.S., 2013. U-Pb zircon geochronology of major lithologic units in the eastern Himalaya: Implications for the origin and assembly of Himalayan rocks. Bulletin, 125(3-4), pp.499-522.

Wells, M., Morton, A. and Frei, D., 2017. Provenance of Lower Cretaceous clastic reservoirs in the Middle East. Journal of the Geological Society, 174(6), pp.1048-1061.

Whitechurch, H., Omrani, J., Agard, P., Humbert, F., Montigny, R. and Jolivet, L., 2013. Evidence for Paleocene–Eocene evolution of the foot of the Eurasian margin (Kermanshah ophiolite, SW Iran) from back-arc to arc: implications for regional geodynamics and obduction. Lithos, 182, pp.11-32.

Wolfe, M.R. and Stockli, D.F., 2010. Zircon (U–Th)/He thermochronometry in the KTB drill hole, Germany, and its implications for bulk He diffusion kinetics in zircon. Earth and Planetary Science Letters, 295(1-2), pp.69-82.

Wrobel-Daveau, J.C., Ringenbach, J.C., Tavakoli, S., Ruiz, G.M., Masse, P. and de Lamotte, D.F., 2010. Evidence for mantle exhumation along the Arabian margin in the Zagros (Kermanshah area, Iran). Arabian Journal of Geosciences, 3(4), pp.499-513.

Xu, J., Stockli, D.F. and Snedden, J.W., 2017. Enhanced provenance interpretation using combined U–Pb and (U–Th)/He double dating of detrital zircon grains from lower Miocene strata, proximal Gulf of Mexico Basin, North America. Earth and Planetary Science Letters, 475, pp.44-57.

Zhang, Z., Xiao, W., Majidifard, M.R., Zhu, R., Wan, B., Ao, S., Chen, L., Rezaeian, M. and Esmaeili, R., 2017. Detrital zircon provenance analysis in the Zagros Orogen, SW Iran: implications for the amalgamation history of the Neo-Tethys. International Journal of Earth Sciences, 106(4), pp.1223-1238.

Ziegler, M. A., 2001. Late Permian to Holocene paleofacies evolution of the Arabian Plate and its hydrocarbon occurrences. GeoArabia, 6(3), pp.445-504.

Competing interests. The authors declare that no competing interest is present.

Author contribution. Renas Koshnaw: Conceptualization, investigation, data collection, writing original draft, reviewing and editing, visualization, funding acquisition. Fritz Schlunegger: Investigation, resources, funding acquisition, reviewing and editing. Daniel Stockli: Investigation, data collection, resources